Cell

Human SNP Links Differential Outcomes in Inflammatory and Infectious Disease to a FOXO3-Regulated Pathway

James C. Lee,[1,2] Marion Espéli,[1,2] Carl A. Anderson,[3] Michelle A. Linterman,[1,2] Joanna M. Pocock,[1,2] Naomi J. Williams,[4] Rebecca Roberts,[5] Sebastien Viatte,[6] Bo Fu,[6,7] Norbert Peshu,[8] Tran Tinh Hien,[9] Nguyen Hoan Phu,[10] Emma Wesley,[11] Cathryn Edwards,[12] Tariq Ahmad,[11] John C. Mansfield,[13] Richard Gearry,[5] Sarah Dunstan,[9,14] Thomas N. Williams,[8,15] Anne Barton,[6] Carola G. Vinuesa,[4] UK IBD Genetics Consortium,[16] Miles Parkes,[2] Paul A. Lyons,[1,2] and Kenneth G.C. Smith[1,2,*]

[1]Cambridge Institute for Medical Research, University of Cambridge, Cambridge Biomedical Campus, Cambridge CB2 0XY, UK
[2]Department of Medicine, University of Cambridge School of Clinical Medicine, Addenbrooke's Hospital, Cambridge CB2 0QQ, UK
[3]Wellcome Trust Sanger Institute, Wellcome Trust Genome Campus, Hinxton, Cambridge CB10 1SA, UK
[4]Department of Pathogens and Immunity, John Curtin School of Medical Research, Australian National University, Canberra ACT 2601, Australia
[5]University of Otago, Department of Medicine, Christchurch 8011, New Zealand
[6]Arthritis Research UK Epidemiology Unit, Manchester Academic Health Science Center, University of Manchester, Manchester M13 9PT, UK
[7]Centre for Biostatistics, Institute of Population Health, University of Manchester, Manchester M13 9PL, UK
[8]Kenya Medical Research Institute/Wellcome Trust Research Program, Centre for Geographic Medicine Research, Kilifi P.O. Box 230-80108, Kenya
[9]Oxford University Clinical Research Unit, Wellcome Trust Major Overseas Program, Hospital for Tropical Diseases, District 5 Ho Chi Minh City, Vietnam
[10]The Hospital for Tropical Diseases, District 5 Ho Chi Minh City, Vietnam
[11]Peninsula College of Medicine and Dentistry, University of Exeter, Exeter EX2 5DW, UK
[12]Department of Gastroenterology, Torbay Hospital, Torquay TQ2 7AA, UK
[13]Institute of Genetic Medicine, Newcastle University, Newcastle NE1 3BZ, UK
[14]Centre for Tropical Medicine, Nuffield Department of Clinical Medicine, University of Oxford, Oxford OX3 7LJ, UK
[15]Department of Medicine, Imperial College, London SW7 2AZ, UK
[16]A full list of The UK IBD Genetics Consortium contributors may be found in the Supplemental Information
*Correspondence: kgcs2@cam.ac.uk
http://dx.doi.org/10.1016/j.cell.2013.08.034

SUMMARY

The clinical course and eventual outcome, or prognosis, of complex diseases varies enormously between affected individuals. This variability critically determines the impact a disease has on a patient's life but is very poorly understood. Here, we exploit existing genome-wide association study data to gain insight into the role of genetics in prognosis. We identify a noncoding polymorphism in *FOXO3A* (rs12212067: T > G) at which the minor (G) allele, despite not being associated with disease susceptibility, is associated with a milder course of Crohn's disease and rheumatoid arthritis and with increased risk of severe malaria. Minor allele carriage is shown to limit inflammatory responses in monocytes via a FOXO3-driven pathway, which through TGFβ1 reduces production of proinflammatory cytokines, including TNFα, and increases production of anti-inflammatory cytokines, including IL-10. Thus, we uncover a shared genetic contribution to prognosis in distinct diseases that operates via a FOXO3-driven pathway modulating inflammatory responses.

INTRODUCTION

Insights obtained from genetic experiments, including genome-wide association studies (GWASs), have substantially advanced our understanding of complex disease biology, and specifically of the processes that drive disease development (Jostins et al., 2012). It is important to remember, however, that disease development is only one aspect of disease biology. Equally important from a clinical standpoint is the biology that determines the course a disease takes following its development (prognosis). Variability in prognosis is observed in most complex diseases and directly impacts upon patient well-being, often to a greater extent than the diagnosis itself. Despite this, the determinants of prognosis in most diseases remain poorly understood and largely unaddressed by those genetic technologies that have yielded such insights into disease development.

This knowledge imbalance is exemplified in Crohn's disease (CD), a chronic, relapsing-remitting form of inflammatory bowel disease thought to be driven by aberrant immune responses to intestinal bacteria. CD has been a major beneficiary of GWAS technology, with over 140 risk loci having been identified (Jostins et al., 2012), though only one of these has been shown to correlate with clinical outcome in CD (Heliö et al., 2003). Such observations have led to criticisms of the utility of GWAS results in translational medicine (McClellan and King, 2010) and raise questions as to whether genetics meaningfully contributes to prognosis in complex disease.

We have recently shown that common transcriptional differences involving the IL-2 and IL-7 cytokine-signaling pathways correlate with prognosis in several diseases, including CD (McKinney et al., 2010; Lee et al., 2011). Here, we perform a candidate gene study to address whether genetic variation in these immune pathways, which have not been associated with the development of CD, might associate with disease prognosis and, if so, to understand the biological mechanisms responsible. To answer this question, we determined that a ''within-cases'' association analysis would be required, in which the genetic profiles of patients with contrasting disease courses could be directly compared. To achieve this, we used a subset of genotype data relating to the IL-2 and IL-7 pathways from an existing GWAS data set (Wellcome Trust Case Control Consortium, 2007) and exploited allied phenotypic data to identify groups of patients with either particularly aggressive or indolent CD. This led to the identification of a noncoding single-nucleotide polymorphism (SNP) in *FOXO3A* that associates with prognosis in CD, despite not being a disease-associated variant (Jostins et al., 2012). *FOXO3A* encodes FOXO3, a member of the forkhead box O family of transcription factors, which also includes FOXO1 and FOXO4 (Accili and Arden, 2004). These proteins are widely expressed and regulate diverse transcriptional programs including cell-cycle control, metabolism, regulatory T cell development, and apoptosis (Burgering and Kops, 2002; Modur et al., 2002; Nakae et al., 2008; Harada et al., 2010; Kerdiles et al., 2010; Ouyang et al., 2010). Although many of these roles are redundant between FOXO family members (Accili and Arden, 2004), FOXO3 has been reported to have nonredundant roles in suppressing inflammatory cytokine production by dendritic cells (Dejean et al., 2009; Watkins et al., 2011) and in limiting the inflammatory sequelae of viral infections (Litvak et al., 2012). Here, we show that during inflammatory responses, in which FOXO3 is exported from the nucleus to the cytoplasm, its reaccumulation in the nucleus is dependent on transcription and de novo protein production, and demonstrate that allelic variation at the prognosis-associated SNP regulates this reaccumulation by controlling *FOXO3A* transcription. Earlier recovery of nuclear FOXO3, which occurs if the indolent disease-associated allele is present, initiates a TGFβ1-dependent pathway in monocytes that reduces production of proinflammatory cytokines, including TNFα, and increases production of the anti-inflammatory cytokine, IL-10—changes consistent with a more indolent disease course. Furthermore, we show that genetic variation at this SNP is also associated with prognosis in rheumatoid arthritis and malaria—other diseases in which these cytokines are implicated. These associations were consistent with the role for these cytokines in each disease, and suggest that this pathway may be generally important in diseases in which these cytokines are involved. Collectively, therefore, these data reveal a pathway by which FOXO3 can abrogate inflammatory responses, and uncover a shared genetic contribution to the prognosis of distinct diseases that impacts upon this pathway and is distinct from the genetic contribution to disease development.

RESULTS

Prognosis-Based Association Study in Crohn's Disease

Subgroups of patients with either particularly aggressive or indolent CD were identified within an existing GWAS cohort (Wellcome Trust Case Control Consortium, 2007) using phenotypic data. Aggressive CD (n = 668) was defined as that for which two or more immunomodulator therapies and/or intestinal resections had been required (treatments reserved for patients with frequently flaring or complicated CD). Indolent CD (n = 389) was defined as disease of greater than 4 years duration, for which immunomodulators or intestinal resections had never been required. Eighty-one genes involved in IL-2 or IL-7 signaling were identified from published literature and pathway libraries (KEGG, Kanehisa and Goto, 2000; Biocarta, http://www.biocarta.com) (Table S1 available online). These pathways were selected because we have previously shown that differences within them correlate with prognosis in several diseases, including CD, and yet unlike a number of other disease-associated cytokines, they have not been implicated in disease development (McKinney et al., 2010; Lee et al., 2011). The allele frequency at 1,134 SNPs within these genes was then compared between the indolent and aggressive CD subgroups (Figure S1). The effect of population structure on the results was assessed by three separate methods and shown to be minimal (genomic control inflation factor 1.04, see Extended Experimental Procedures). Replication of the three most significant associations was then sought in three independent cohorts, each similarly divided into indolent and aggressive cases (Table S2). The prognostic association of rs12212067, an intronic SNP within *FOXO3A*, was replicated in all three cohorts, with the minor (G) allele being consistently more common in patients with indolent CD (combined p value = 2.1×10^{-8}, Tables 1 and S3). Notably, this SNP was not associated with risk for CD either in the GWAS used for this study (p = 0.88)—a sample of 1,748 cases and 2,938 controls (Wellcome Trust Case Control Consortium, 2007)—or in a larger meta-analysis (p = 0.99) of 6,333 cases and 15,056 controls (Franke et al., 2010), which suggests that if it does influence disease risk, its effect size is negligible.

rs12212067 Regulates Transcription of FOXO3A during Inflammation

To investigate how genetic variation at this locus might influence prognosis in CD, we first examined whether rs12212067 was in linkage disequilibrium (LD) with a coding variant that could affect protein structure or function. Using sequence data from the 1000 Genomes Project Consortium et al. (2010) we identified all of the SNPs in LD ($r^2 > 0.5$) with rs12212067, but none of these were exonic (Table S4 and Figure S2). Indeed, of the 45 coding variants that have been described within *FOXO3A* (dbSNP,

Table 1. Association of rs12212067 with Prognosis in CD

Cohort	n[a]	MAF (Aggressive)	MAF (Indolent)	Odds Ratio (95% CI)	p Value
Primary cohort (WTCCC CD GWAS)	1,057 (668, 389)	0.084	0.131	0.61 (0.46–0.83)	6.16×10^{-4}
Replication cohort 1 (UK - TaqMan)	701 (344, 357)	0.094	0.129	0.71 (0.49–1.00)	0.025
Replication cohort 2 (NZ - TaqMan)	226 (136, 90)	0.070	0.128	0.51 (0.26–1.02)	0.029
Replication cohort 3 (UK - Immunochip)	1,001 (670, 331)	0.083	0.133	0.59 (0.44–0.81)	6.50×10^{-4}
Combined analysis	2,985 (1,818, 1,167)	0.084	0.131	0.62 (0.52–0.73)	2.09×10^{-8}

Aggressive CD, patients requiring ≥ two immunomodulators and/or intestinal resections; Indolent CD, patients with > 4 years follow-up, no immunomodulators or intestinal resections. p values calculated with Cochran-Armitage test (primary cohort) and Fisher's exact test (replication cohorts and combined analysis). Odds ratios refer to the minor (G) allele and aggressive Crohn's disease (CD). WTCCC, Wellcome Trust Case Control Consortium; UK, United Kingdom, NZ, New Zealand, MAF, minor allele frequency; CI, confidence interval. See also Figure S1 and Tables S1, S2, S3, S4.
[a]Total sample size (Aggressive, Indolent).

http://www.ncbi.nlm.nih.gov/projects/SNP) none were in any demonstrable LD with rs12212067: T > G (r2 < 0.001, data not shown). This implies that noncoding variation is likely to drive the association. The majority of complex disease-associated SNPs are also noncoding and are assumed to affect gene expression, though in most cases this has not been confirmed (McClellan and King, 2010). To ascertain whether rs12212067: T > G, or a variant in strong LD with it, might influence gene expression, we used a clone based allele-specific expression assay to analyze *FOXO3A* transcription in monocytes from heterozygous individuals (obtained from a genotype-selectable bioresource; http://www.cambridgebioresource.org.uk). This facilitates a direct comparison between the amount of *FOXO3A* pre-mRNA that is transcribed from each allele or haplotype and ensures that external factors affect both alleles equally. Under basal (unstimulated) conditions, the ratio of major (T) to minor (G) alleles in *FOXO3A* pre-mRNA was no different to that observed in genomic DNA (in which it is inherently 1:1), indicating that allele-specific expression did not occur. However, following stimulation with lipopolysaccharide (LPS), a toll-like receptor 4 (TLR4) ligand, we observed consistent allele-specific differences in transcription, with over twice as much *FOXO3A* being transcribed from the DNA strand containing the minor G allele (associated with indolent CD) than from the strand containing the major T allele (Figure 1A).

Genetic Variation at rs12212067 Modulates Inflammatory Cytokine Production by Monocytes

To determine whether this difference in *FOXO3A* transcription had functional consequences, we stimulated peripheral blood mononuclear cells (PBMC) from healthy individuals, who were homozygous for either the minor or major allele at rs12212067, and measured cytokine production. We initially focused upon TNFα, the archetypal proinflammatory cytokine in CD (Khor et al., 2011) and target of the most effective medical therapy (Krygier et al., 2009); and IL-10, an anti-inflammatory cytokine, which when deleted produces one of the best mouse models of IBD (Rennick et al., 1997); and genetic variants of which are associated with CD (Jostins et al., 2012). Following LPS stimulation, we observed striking genotype-specific differences in the production of these cytokines, with PBMC from minor (G) allele homozygotes secreting less TNFα than those from major (T) allele homozygotes. PBMC from minor allele homozygotes also secreted relatively more IL-10 in response to higher concentrations of LPS (Figure 1B). This pattern of cytokine production implies that, under these conditions, minor allele homozygotes generate lesser inflammatory responses. There were no genotype-specific differences in the proportion, activation status or immunophenotype of leukocyte subsets within PBMC that could explain this result (Table S5). These included regulatory T cells and dendritic cells, in which FOXO3 has specific roles (Dejean et al., 2009; Kerdiles et al., 2010).

To ascertain which cell population was responsible for the differences in cytokine production, we used flow cytometry to identify the TNFα and IL-10 producing cells. Following stimulation with LPS (100 ng/ml), production of both cytokines could be detected within $CD14^+$ monocytes, but not within $CD3^+$ T cells or $CD19^+$ B cells (Figure 1C). Of note, differences were again observed between the genotypes, with less TNFα and more IL-10 being produced by monocytes from minor allele homozygotes (Figure S3). To determine whether this phenomenon was cell-intrinsic or due to another cell type influencing monocyte cytokine production, we purified monocytes and stimulated them in isolation. Despite removing the influence of other cell types, we observed the same genotype-specific differences in cytokine production (Figure 1D), implying that the effect was monocyte intrinsic. We then examined whether the differences were specific to stimulation via TLR4 or would also occur with other TLR ligands (Pam3Cys4 [TLR1/2], Poly(I:C) [TLR3], Flagellin [TLR5], and CpG [TLR9]). We observed the same reciprocal differences in TNFα and IL-10 production in response to all of these ligands except Poly(I:C), which induced little TNFα and IL-10 production consistent with previous reports (Lundberg et al., 2007) (Figure 1E). Thus, the genotype-specific differences in cytokine production arise from monocytes but can be induced by several pathogen-associated molecular patterns.

We then examined the production of other proinflammatory cytokines to determine whether these also differed by genotype. We quantified GM-CSF, IL-1β, IL-2, IL-4, IL-5, IL-6, IL-8, and IL-12p40 and observed that, as well as producing less TNFα, monocytes from minor (G) allele homozygotes also produced less IL-1β, IL-6, and IL-8 compared to those from major (T) allele homozygotes (Figures 1F and S4). Notably, these cytokines constitute a major part of the innate immune response to pathogens (Auffray et al., 2009) and can influence the phenotype of T cells (Dejean et al., 2009).

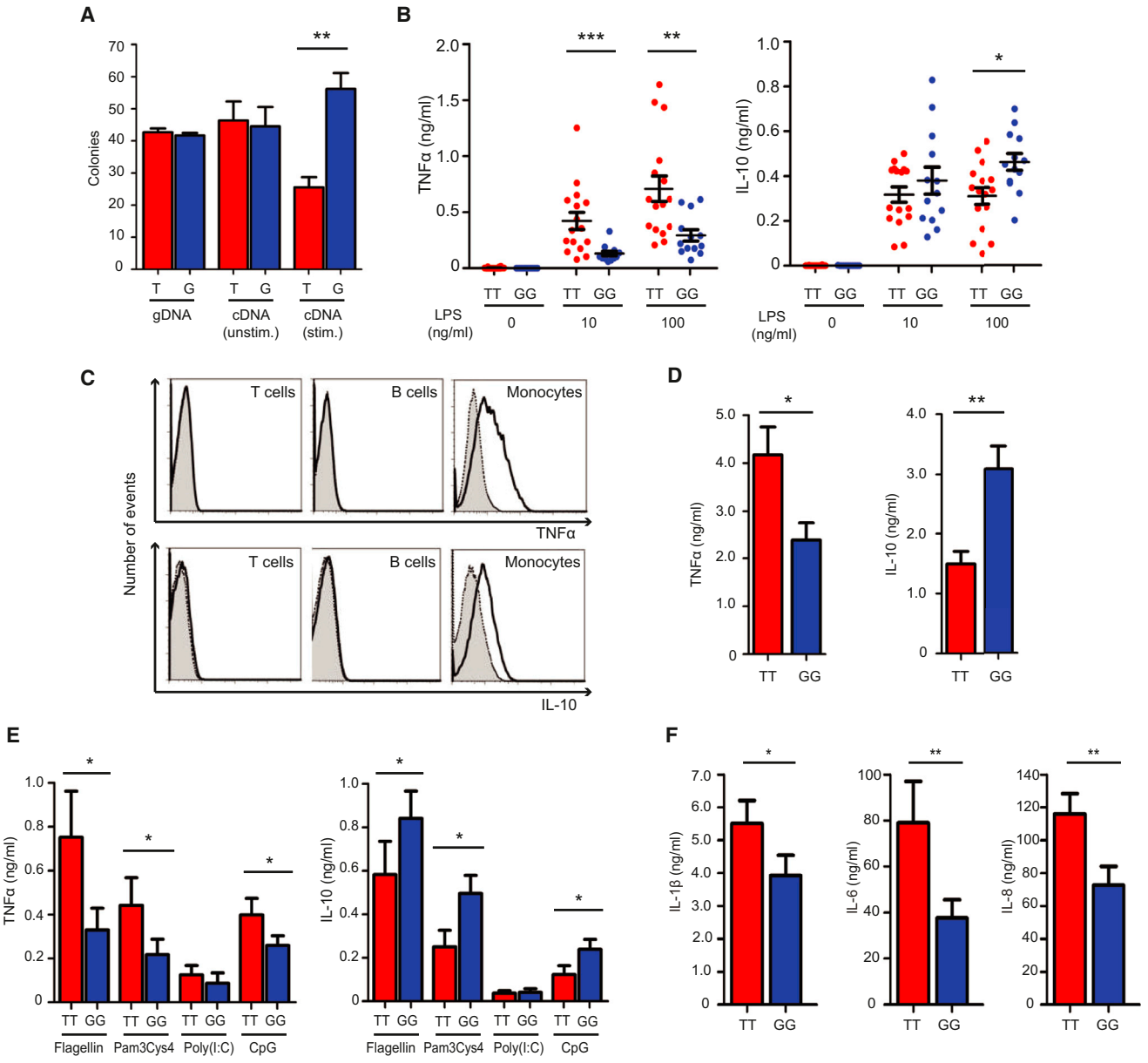

Figure 1. Genotype at rs12212067 Drives Allele-Specific Expression of *FOXO3A* and Modulates Inflammatory Cytokine Production in Monocytes

(A) Allele-specific expression assay showing the ratio of rs12212067 alleles in genomic DNA (gDNA) and complementary DNA (cDNA; synthesized from pre-mRNA) from peripheral monocytes of heterozygous individuals. Ninety-six colonies were genotyped per individual per condition (either unstimulated [unstim.] or stimulated with 100 ng/ml LPS [stim.]); n = 6.

(B) TNFα and IL-10 production by PBMC from minor (G) and major (T) allele homozygotes at rs1221267 following 24 hr stimulation with LPS; n = 15 per group, assayed in triplicate.

(C) Intracellular staining of TNFα and IL-10 production in LPS-stimulated (100 ng/ml) $CD3^+$ T cells, $CD19^+$ B cells and $CD14^+$ monocytes. Isotype control shown as shaded histogram. Results representative of 20 experiments.

(D) TNFα and IL-10 production by purified monocytes from minor and major allele homozygotes following 24 hr stimulation with LPS (100 ng/ml); n = 11 per group, assayed in triplicate. 20 of these individuals had provided samples used in B.

(E) TNFα and IL-10 production by PBMC from minor and major allele homozygotes following 24 hr stimulation with other TLR ligands; n = 11 per group (same individuals' samples as D), assayed in triplicate.

(F) IL-1β, IL-6, and IL-8 production by purified monocytes from minor and major allele homozygotes following 24 hr stimulation with LPS (same samples as in D), n = 11 per group. Data are represented as mean ± SEM, *p < 0.05, **p < 0.01, ***p < 0.001.

See also Figures S2, S3, S4 and Tables S4 and S5.

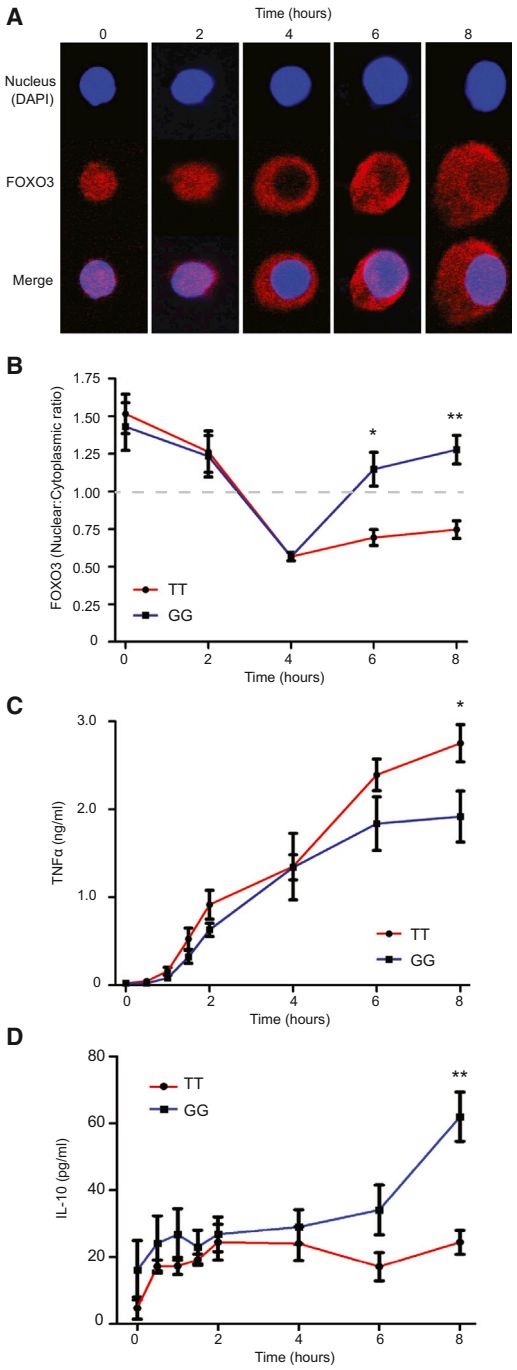

Figure 2. Genotype at rs12212067 Influences the Nuclear Recovery of FOXO3 during Cellular Activation

(A) The subcellular localization of FOXO3 in monocytes during LPS stimulation (representative images). FOXO3 (red) and nucleus (DAPI, blue).

(B) The ratio of nuclear to cytoplasmic FOXO3 over time (mean immunofluorescence intensity) in LPS-stimulated monocytes from minor (G) and major (T) allele homozygotes at rs12212067 (100 ng/ml, n = 10). The dotted line indicates transition from higher signal in nucleus (above) to cytoplasm (below).

(C–D) Production of TNFα (C) and IL-10 (D) by monocytes analyzed in (B). Cytokines were quantified in triplicate by ELISA. Data are represented as mean ± SEM, *$p < 0.05$, **$p < 0.01$.

See also Figure S5.

Differences in FOXO3A Transcription during Inflammation Determine when FOXO3 Reaccumulates within the Nucleus

We next considered how differences in *FOXO3A* transcription might affect cytokine production. Because the downstream transcriptional program of FOXO3 is largely controlled by posttranslational modifications that determine whether it is retained within, or excluded from, the nucleus (Hedrick, 2009), we first examined how the intracellular localization of FOXO3 changed as monocytes were stimulated (Figure 2A). TNFα and IL-10 production were also measured. We showed that in unstimulated monocytes, most FOXO3 was nuclear, and TNFα production was low. Upon LPS stimulation, FOXO3 was translocated out of the nucleus (Figure 2A) and a linear increase in TNFα production was observed. This process occurred similarly in minor and major allele homozygotes, until very little nuclear FOXO3 remained after 4 hr (Figure 2B). Thereafter, a gradual increase in the amount of nuclear FOXO3 was observed (termed "nuclear recovery"), which correlated with reduced TNFα and increased IL-10 production. Strikingly, this nuclear recovery phase occurred considerably faster in minor (G) allele homozygotes than in major (T) allele homozygotes and correlated with an earlier reduction in TNFα production and an earlier increase in IL-10 production (Figures 2B–2D). This difference is consistent with the allele-specific expression differences and implies that, during inflammation, increased *FOXO3A* transcription in carriers of the minor (G) allele leads to faster recovery of nuclear FOXO3. This also suggests that de novo protein synthesis, rather than nuclear translocation of cytoplasmic FOXO3, is responsible for nuclear recovery; consistent with the observation that once FOXO3 is translocated into the cytoplasm, it is targeted for proteasomal degradation (Yang et al., 2008). This was confirmed by showing that if protein synthesis was inhibited, nuclear recovery of FOXO3 was substantially retarded (Figure S5).

The Effect of rs12212067 on Monocyte Cytokine Production Is TGFβ1 Dependent

Next we investigated how the earlier recovery of nuclear FOXO3 might alter inflammatory cytokine production. In mice, silencing *Foxo3a* has been shown to abrogate production of TGFβ1 (Watkins et al., 2011), an anti-inflammatory cytokine that can modulate production of other cytokines (Musso et al., 1990; Fadok et al., 1998). To determine whether TGFβ1 might contribute to the observed differences in cytokine production, we re-examined the supernatants from the earlier experiments. We found that relatively more TGFβ1 had been secreted by PBMC and monocytes from minor (G) allele homozygotes (Figure 3A) with the greatest difference, and highest concentrations, being present in the monocyte supernatants—implicating these cells as the major source of TGFβ1. To determine whether this difference might contribute to the differences in TNFα and IL-10 production, we examined the effects of blocking TGFβ1 signaling. Strikingly, we observed that the genotype-specific differences in TNFα and IL-10 production were abolished if TGFβ1 signaling was inhibited (Figure 3B)—suggesting that a TGFβ1-dependent mechanism was responsible. In support of this, differences in TGFβ1 titers from minor and major allele homozygotes were also detected in the samples from the earlier time-course experiment, with the kinetics of TGFβ1 production correlating with the differences

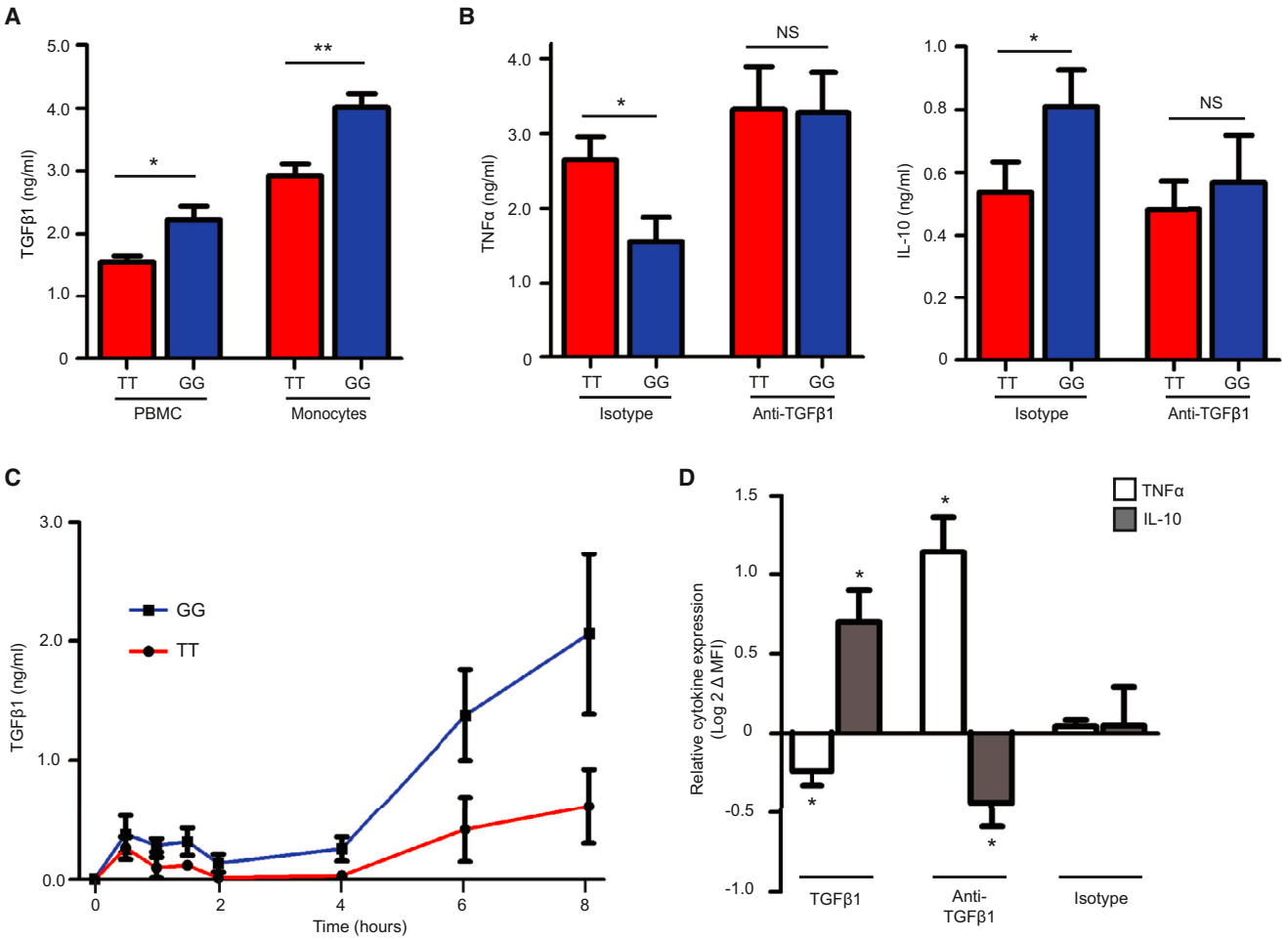

Figure 3. A TGFβ1-Dependent Mechanism Is Responsible for the Effect of rs12212067 on Monocyte Cytokine Production

(A) TGFβ1 production by PBMC (n = 20 per group) and monocytes (n = 13 per group) from minor (G) and major (T) allele homozygotes at rs1221267 following 24 hr stimulation with LPS (100 ng/ml), assayed in triplicate.

(B) TNFα and IL-10 production by PBMC from minor and major allele homozygotes following 24 hr stimulation with LPS (100 ng/ml) in the presence of a TGFβ1-neutralizing antibody or isotype control; n = 10 per group, assayed in triplicate.

(C) Production of TGFβ1 by monocytes in the time-course experiment shown in Figure 2, measured in triplicate by ELISA.

(D) The effect of TGFβ1 or a TGFβ1-neutralizing antibody upon TNFα and IL-10 production by LPS-stimulated monocytes, assessed using flow cytometry (mean fluorescence intensity, MFI). Data are $\log_2$ transformed following normalization, Wilcoxon signed-rank test; n = 6. Data are represented as mean ± SEM, *p < 0.05, **p < 0.01, NS, nonsignificant.

in nuclear recovery of FOXO3 (Figure 3C). Moreover, the addition of exogenous TGFβ1 to stimulated monocytes of either genotype led to less TNFα and more IL-10 production—consistent with the differences observed between the genotypes—whereas blockade of TGFβ1 had the opposite effect (Figure 3D). This suggests that endogenous TGFβ1 production plays an important regulatory role in monocyte-driven inflammatory responses.

FOXO3 Regulates TGFβ1 Production in Stimulated Monocytes

Although these data implicate a TGFβ1-dependent mechanism in driving the genotype-specific differences in cytokine production, it was unclear how the earlier recovery of nuclear FOXO3 might mediate this. To determine whether FOXO3 directly regulated TGFβ1 production, we analyzed the *TGFβ1* promoter and identified several sites at which FOXO3 was predicted to bind (Figure 4A and Table S6). To establish whether this interaction occurred during monocyte activation, we immunoprecipitated FOXO3 from stimulated monocytes and found that the DNA to which it was bound included the predicted binding site from the *TGFβ1* promoter (Figure 4B), confirming that a direct protein-DNA interaction occurs. To determine the result of this interaction, we silenced *FOXO3A* in two monocyte cell lines, U937 (Sundström and Nilsson, 1976) and MONO-MAC6 (Ziegler-Heitbrock et al., 1988), and examined the effect on *TGFβ1* transcription. In both, we showed that when *FOXO3A* was silenced, transcription from the *TGFβ1* promoter was reduced, confirming that the FOXO3-*TGFβ1* interaction promotes *TGFβ1* transcription (Figure 4C). Together, these data reveal that FOXO3 induces *TGFβ1* expression via a direct protein-DNA interaction in

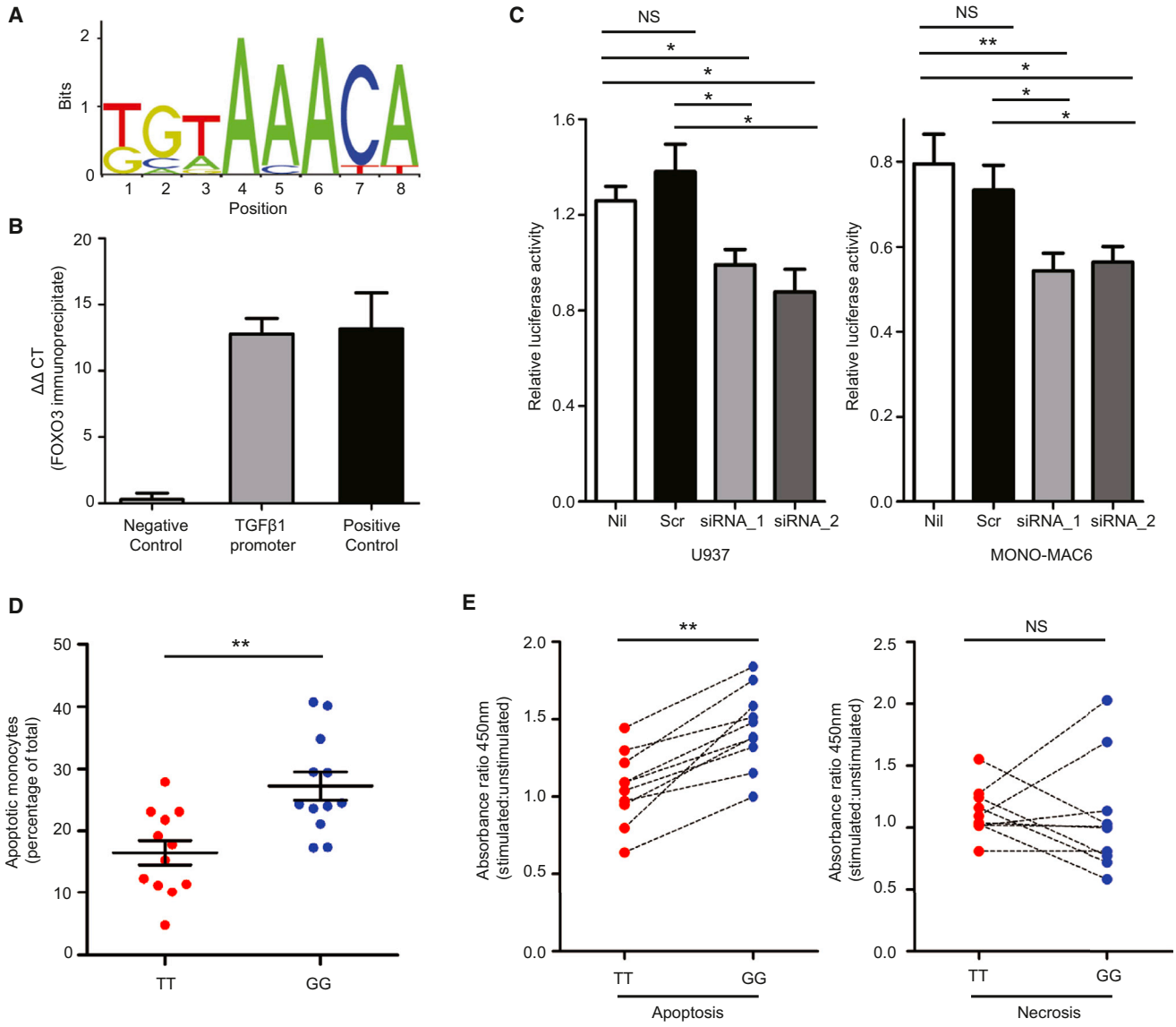

Figure 4. FOXO3 Regulates TGFβ1 Production in Stimulated Monocytes

(A) Jaspar sequence logo of the FOXO3-binding site (http://jaspar.genereg.net).

(B) ChIP-qPCR analysis of the *TGFβ1* promoter following FOXO3 immunoprecipitation. Enrichment for each region is shown relative to input (5 ng) and normalized against the results of a negative control immunoprecipitate (polyclonal IgG). Validated positive and negative control genomic regions were used. Controls shown are *HBB* (negative) and a region upstream of *MSTN* (positive). n = 3.

(C) Luciferase reporter assay showing effect of silencing *FOXO3A* on transcription from the *TGFβ1* promoter in two monocyte cell lines (U937 and MONO-MAC6). No transfection (Nil) and scrambled controls (Scr) are shown. Data representive of three experiments, each with seven biological replicates.

(D) Apoptosis in monocytes from minor (G) and major (T) allele homozygotes at rs12212067 following 24 hr stimulation with LPS (100 ng/ml); assessed by flow cytometry (7-AAD$^+$, Annexin V$^+$), n = 12 per group.

(E) The change in the concentration of mono- and oligonucleosomes in the cytoplasm (apoptosis) and supernatant (necrosis) of monocytes following LPS stimulation (24 hr, 100 ng/ml), assessed in triplicate by ELISA. Dotted lines link paired samples; Wilcoxon signed-rank test, n = 8 per group. Data are represented as mean ± SEM, *p < 0.05, **p < 0.01, NS, nonsignificant.

See also Figure S6 and Table S6.

stimulated monocytes and explain how the earlier recovery of nuclear FOXO3 could modulate TNFα and IL-10 production in a TGFβ1-dependent manner.

TGFβ1 has also been implicated in the modulation of immune responses by apoptotic cells (Fadok et al., 1998), whereas FOXO3 is known to be proapoptotic (Brunet et al., 1999). This raised the possibility that earlier nuclear recovery of FOXO3 might also augment TGFβ1 production indirectly via apoptosis induction. To examine this, we quantified apoptosis in PBMC following LPS stimulation (using Annexin V and 7-AAD) and

observed that more occurred in minor (G) allele homozygotes (Figure 4D), consistent with the earlier recovery of nuclear FOXO3 in this genotype. To exclude a contribution from necrotic cells to this result, we quantified mono- and oligonucleosomes in the supernatant (necrosis) and cytoplasm (apoptosis) of PBMC from another cohort of minor and major allele homozygotes and again observed more apoptosis in minor allele homozygotes following stimulation (Figure 4E). We also confirmed that stimulated monocytes produced less TNFα and more IL-10 in the presence of autologous apoptotic cells and that this could be abrogated by TGFβ1-blockade (Figure S6). These data imply that FOXO3 might drive TGFβ1 production not only via a direct interaction with its promoter, but also indirectly via the control of apoptosis.

FOXO3 has also been shown to mediate some of the downstream components of TGFβ1 signaling (Wildey and Howe, 2009), raising the possibility that earlier nuclear recovery might amplify some of the effects of TGFβ1 production. However, we did not detect any genotype-specific differences in the transcription of 11 genes whose activation by TGFβ1 is FOXO dependent (Gomis et al., 2006) (data not shown), consistent with reports that this role is redundant between FOXO family members (Seoane et al., 2004).

Foxo3 Deficiency Leads to Increased Disease Severity in a Mouse Model of Colitis

Collectively, these data provide a plausible mechanism to explain the association of the haplotype tagged by rs12212067 with prognosis in CD, particularly given the role that circulating monocytes and their intestinal derivatives play in CD pathogenesis (Geissmann et al., 2010; Khor et al., 2011; Bain et al., 2013). To provide further evidence of how altered FOXO3 function might influence intestinal inflammation, we used an in vivo model of inflammatory bowel disease. Using dextran sodium sulfate (DSS), we induced colitis in mice harboring a missense mutation in the highly conserved Forkhead DNA-binding domain of *Foxo3*, known to abrogate its function (*Foxo3a*$^{MommeR1/MommeR1}$ mice—from here termed *Foxo3a*$^{-/-}$, Youngson et al., 2011) and compared the severity of the resulting disease with that observed in heterozygous (*Foxo3a*$^{+/-}$) and wild-type mice (*Foxo3a*$^{+/+}$). We showed that, consistent with the in vitro data, reduced *Foxo3a* transcriptional activity predisposed to a more severe colitis. This was evident histologically (Figures 5A and 5B) and by greater losses in body weight (Figure 5C), increased colonic weight, and reduced colonic length (Figures 5D and 5E). Moreover, the colitis in *Foxo3a*$^{-/-}$ mice was characterized by increased expression of proinflammatory cytokines and reduced expression of IL-10 in the diseased colons, which mirrored our in vitro data (Figures 5F and S7). Importantly, these differences could not be solely attributed to an increase in activated myeloid cells within the colon, as they were still present after normalization against CD11b, a myeloid activation marker (Figure 5F).

Genetic Variation in FOXO3A Is Associated with Prognosis in Rheumatoid Arthritis and Malaria

The pathway we have identified—by which genetic variation in *FOXO3A* can modulate inflammatory cytokine production in monocytes—would not only be expected to influence the outcome of CD, but also of other diseases involving these cytokines. Rheumatoid arthritis (RA) is a chronic inflammatory polyarthritis, in which autoimmune-mediated synovial inflammation can lead to progressive joint destruction and disability. The pathogenesis of RA involves many cytokines, including TNFα, IL-6, and IL-10, with blockade of the first two being effective therapies (Feldmann and Maini, 2008). We therefore genotyped rs12212067 in two prospectively collected cohorts of RA patients, who had had serial radiographs of their hands and feet at regular intervals (Symmons and Silman, 2003; James et al., 2004), and examined whether the rs12212067: T > G haplotype was associated with clinical outcome. Of note, this SNP has not been associated with susceptibility to RA (Wellcome Trust Case Control Consortium, 2007). We confirmed that the minor (G) allele, which associated with milder CD, was also associated with a milder course of RA, characterized by less joint damage over time (equivalent to a reduction of 1.5 Larsen units per copy of the G allele) (Tables 2 and S7). This is consistent with the functional effects of allelic variation at this SNP and suggests that prognosis in RA is also influenced by FOXO3-dependent control of inflammatory responses.

Aside from their involvement in inflammatory disease, cytokines such as TNFα, IL-6, and IL-10 also participate in immune responses to infection. During initial infection with malaria—the leading cause of childhood death in Africa—proinflammatory cytokines, including TNFα, are released by monocytes and macrophages to help kill parasites (Malaguarnera and Musumeci, 2002), whereas IL-10 inhibits this protective response (Hugosson et al., 2004). We hypothesized that the effects of rs12212067: T > G would impair parasite clearance and increase the risk of severe malaria. To test this, we genotyped rs12212067 in separate cohorts of Kenyan (Williams et al., 2005) and Vietnamese patients (Tran et al., 1996) who were admitted to hospital with severe *P. falciparum* malaria and ethnically matched controls. In both cohorts, we found an association between the minor (G) allele and increased susceptibility to severe malaria (Tables 2 and S3), consistent with the predicted result of producing less TNFα and more IL-10 during initial infection.

DISCUSSION

Despite advances in complex disease genetics, remarkably little attention has been paid to whether genetics contributes to aspects of disease biology beyond simple susceptibility. Here, we identify a genetic variant in *FOXO3A* that associates with the prognosis, but not diagnosis, of three distinct diseases; CD, RA, and malaria. This observation has important implications for how we think about the genetics of complex disease and introduces the concept that common variants can determine the outcome of one or more diseases, without being associated with the disease itself. By focusing more attention on this aspect of disease biology, it may be possible to uncover new therapeutic targets that are relevant in several diseases and also facilitate the development of personalized medicine, both through more accurate prediction of outcome and better targeted therapies.

FOXO3 has been linked to the regulation of immune responses using systems biology (Litvak et al., 2012) and knockout mouse models (Dejean et al., 2009), although whether this was relevant

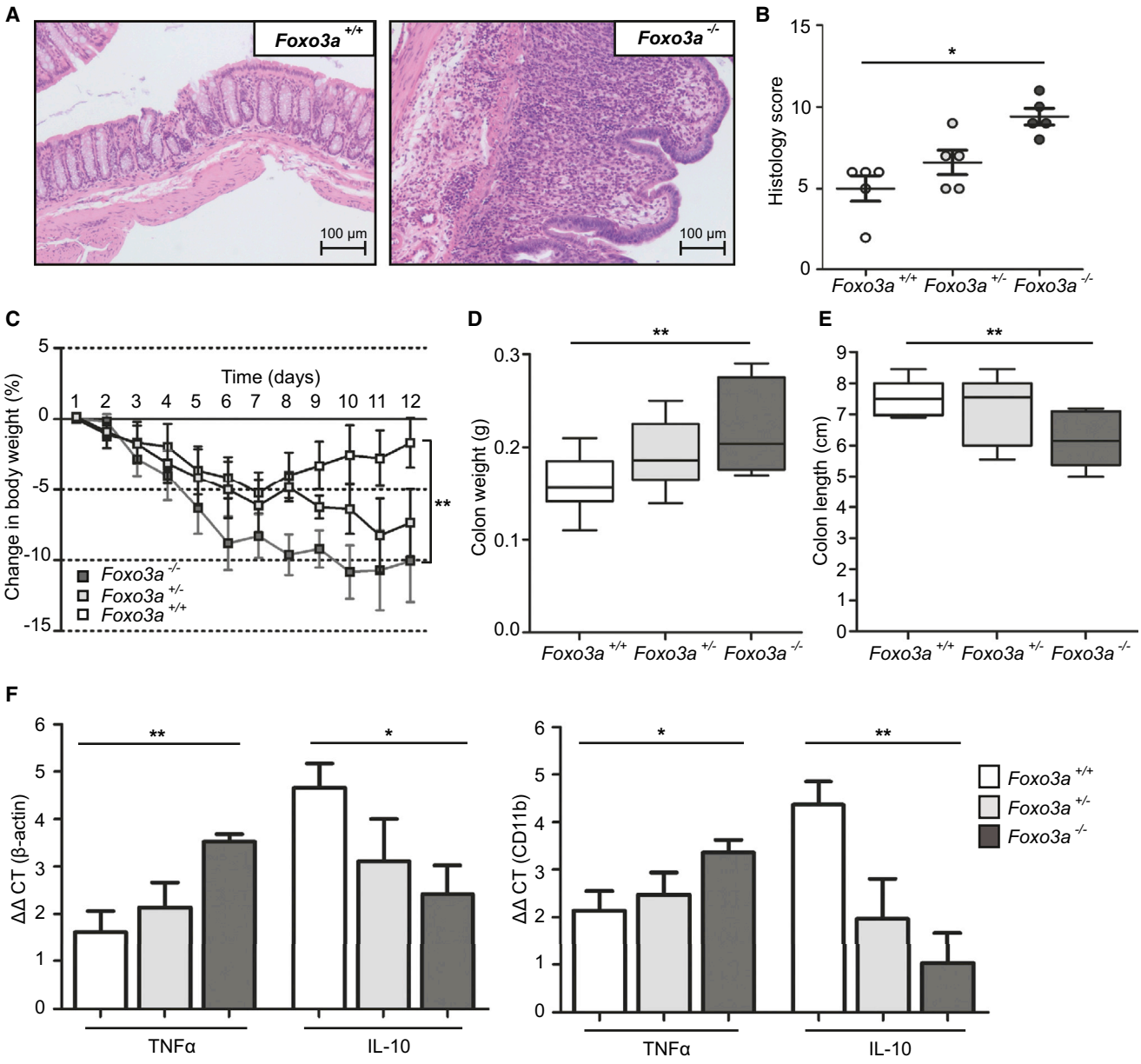

Figure 5. Loss of *Foxo3a* Activity Predisposes to More Severe Colitis in a Mouse Model

(A–F) Colitis was induced in littermate *Foxo3a*$^{-/-}$, *Foxo3a*$^{+/-}$, and *Foxo3*$^{+/+}$ mice using 2% DSS (7 d). Results representative of two experiments each with 5 mice per group, Mann Whitney test unless indicated. Data are represented as mean ± SEM, *$p < 0.05$, **$p < 0.01$.

(A) Light microscopy of H&E stained colonic sections from *Foxo3a*$^{-/-}$ and *Foxo3*$^{+/+}$ mice. Colons removed on day 12.

(B) Histological assessment of colitis severity, scored with a standard tool (Dieleman et al., 1998).

(C) Percentage change in total body weight (measured daily). Two-way ANOVA.

(D) Colon weight (day 12).

(E) Colon length (day 12).

(F) Quantitative PCR of TNFα and IL-10 mRNA extracted from paraffin-embedded colonic sections. Normalization to beta-actin (left) and CD11b (right).

See also Figure S7.

in human disease, or even occurred physiologically in humans, was unclear. By exploring the effects of the prognosis-associated variant, we have identified a pathway by which FOXO3 limits inflammatory responses in human monocytes through a paracrine TGFβ1-dependent mechanism and have confirmed the importance of this pathway in an in vivo model. This, therefore, not only provides a molecular explanation for the association of rs12212067: T > G with prognosis in each disease, but also sheds light on the role of FOXO3 in regulating monocyte-driven inflammation.

Table 2. The Minor, G, Allele at rs12212067 Is Associated with Indolent RA but Increased Risk of Severe Malaria

	Rheumatoid Arthritis							*P. falciparum* Malaria						
	Norfolk Arthritis Register[a] (1,071 RA Patients)				Early Rheumatoid Arthritis Study[a] (382 RA Patients)			Kenyan Cohort (1,340 Severe Cases, 2,436 Controls)			Vietnamese Cohort (223 Severe Cases, 653 Controls)			Meta-Analysis (Malaria)
Phenotype	Year 0 MAF (n = 306)	Year 2 MAF (n = 242)	Year 5 MAF (n = 423)	p	Year 0 MAF (n = 366)	Year 2 MAF (n = 349)	Year 4 MAF (n = 210)	p	MAF	OR	P	MAF	OR	p	p_{meta}
Severe disease	0.09	0.10	0.09	0.004	0.10	0.09	0.10	0.004	0.25	1.13	0.017	0.25	1.35	0.014	0.001
Mild disease (RA) or controls (malaria)	0.09	0.14	0.14	-	0.09	0.12	0.13	-	0.22	-	-	0.20	-	-	-

Indolent RA, complete absence of radiological damage in hands and feet, including joint space narrowing (Larsen score = 0). Severe RA, presence of radiological damage in hands or feet (Larsen score > 0). Severe malaria, *P.falciparum* parasitemia complicated by features of severe malaria, requiring hospital admission. Malaria controls, ethnically matched from same region. One-tailed p values calculated using Fisher's exact test for malaria cohorts, and Generalized Linear Latent and Mixed Modeling for RA cohorts (this considers disease duration and Larsen score as continuous variables to incorporate multiple records per patient over time). OR refer to the minor (G) allele and severe disease. MAF, minor allele frequency;OR, odds ratio; p_{meta}, meta-analysis of malaria cohorts. See also Tables S3 and S7.

[a]Data are presented from a subset of time points. Analysis of statistical significance incorporated all time points for which data were available (including some not shown—see Table S7). As Larsen score was considered a continuous variable for the analysis, the mild and aggressive groups shown are illustrative of the differences in MAF but were not directly compared to determine statistical significance.

It is noteworthy that the prognostic association of this polymorphism appears to be mediated via monocytes, which are known to be important in these inflammatory and infectious diseases (Malaguarnera and Musumeci, 2002; Khor et al., 2011; Bain et al., 2013; Davignon et al., 2013). CD pathogenesis, for example, is thought to stem from a dysfunctional innate immune response to intestinal bacteria by proinflammatory macrophages and dendritic cells (Khor et al., 2011)—both of which derive from circulating monocytes (Geissmann et al., 2010; Rivollier et al., 2012; Bain et al., 2013). The resulting production of proinflammatory cytokines by these cells not only drives disease activity but is also the target of the most effective therapy (Krygier et al., 2009). Similarly, in RA, disease severity correlates with the extent of synovial infiltration by monocytes/macrophages, and these can be targeted therapeutically (Mulherin et al., 1996; Davignon et al., 2013).

Although our evidence points to an effect in monocytes, T cells are also important in these diseases (Feldmann and Maini, 2008; Khor et al., 2011). However, we did not detect any differences in T cell phenotype in our experiments. This does not exclude a T cell effect in vivo, but even if one was seen, it may be secondary to FOXO3-driven differences in cytokine production. This is exemplified in infected *Foxo3* deficient mice (a strain derived independently of the *Foxo3*^{MommeR1} mice) where the resulting T cell phenotype is due to enhanced inflammatory cytokine production by myeloid cells (Dejean et al., 2009).

The importance of the FOXO3-driven pathway that we describe, and its genetic regulation, may not only be limited to disease. Several key elements of this pathway have been independently associated with human longevity, including polymorphisms in *FOXO3A* (Kenyon, 2010) and lesser inflammatory responses—characterized by less TNFα and more IL-10 production (Licastro et al., 2005). Whether the control of inflammatory cytokine production by FOXO3 links these observations and thereby influences lifespan is unknown but warrants further investigation.

To date, over 1,000 GWASs have been performed to study the role of genetics in disease susceptibility (Hindorff et al., 2013), but very few have been re-examined since their initial publication. Our data demonstrate that further insights into disease biology can be obtained using such data sets, and highlight the potential to discover pathways that may be critically important in disease biology but which were not revealed by the same index studies.

In summary, therefore, we show that the role of genetics in complex disease extends beyond a contribution to disease development and describe a FOXO3-dependent pathway that limits inflammatory responses and which, through its genetic regulation, is independently associated with the prognosis of distinct inflammatory and infectious diseases.

EXPERIMENTAL PROCEDURES

GWAS Reanalysis

Single-marker allelic association analysis was performed using post-QC genotype calls (Wellcome Trust Case Control Consortium, 2007) for 1,134 SNPs within 81 genes implicated in IL-2 or IL-7 signaling (including 2 kb on either side to encompass regulatory regions). Data were analyzed in PLINK (http://pngu.mgh.harvard.edu/~purcell/plink) using Cochran-Armitage tests to determine

statistical significance. Genotype frequencies were in Hardy Weinberg equilibrium ($p > 0.05$). The contribution of population structure to the association results was assessed using *structure* (Pritchard et al., 2000a), the Genomic Control method and a Breslow-Day test. Replication was sought in three independent replication cohorts. See also Extended Experimental Procedures.

Genotyping

Non-GWAS genotyping was performed using TaqMan predesigned SNP genotyping assays (Applied Biosciences), a custom genotyping chip (Illumina Immunochip), or Sequenom MassArray technology, as indicated.

Cambridge BioResource

In vitro experiments were performed using blood samples from healthy volunteers, selected by genotype from a human bioresource (Cambridge BioResource, http://www.cambridgebioresource.org.uk). All provided informed consent. Samples were paired and age and sex matched. Investigators were blinded to sample genotype until study completion. Ethical approval was obtained from Cambridgeshire Regional Ethics Committee.

Allele-Specific Expression

A clone-based allele-specific expression assay (Rainbow et al., 2008) was performed using monocytes from six individuals heterozygous at rs12212067. Genomic DNA and pre-mRNA were extracted and amplified, and allelic ratios assessed by colony genotyping (TaqMan, 96 colonies per individual per condition).

Cell Stimulations

Aliquots of 1×10^6 cells/ml were stimulated in Complete RPMI at 37°C, 5% CO_2. 50 μl of each stimulus (or control) was used to produce the final concentrations. Cytokines were quantified in triplicate using cytometric bead arrays (BD), ELISAs (Quantikine, R&D Systems) or MesoScale Discovery immunoassays (see Extended Experimental Procedures).

Immunofluorescence

Stimulated monocytes were fixed (4% PFA), blocked (2% gelatin), and stained with anti-FOXO3 (Cell Signaling) conjugated to an AF594 secondary antibody. Nuclear staining was performed using Hoechst dye. Images were captured on a Zeiss LSM510 META Confocal Microscope and analyzed with Volocity software (Perkin Elmer).

ChIP-qPCR

Chromatin from stimulated monocytes was sheared by water-bath sonication (Bioruptor, Diagenode) and FOXO3 was immunoprecipitated with a ChIP-grade anti-FOXO3 antibody (Abcam). Polyclonal IgG was used as a negative control. Quantitative (q)PCR was performed for a region of the *TGFβ1* promoter predicted to contain a FOXO3-binding site, along with six positive and five negative controls (all previously validated in Eijkelenboom et al., 2013). Input DNA was standardized (5 ng) and the data normalized to the results obtained using a polyclonal IgG immunoprecipitation.

Luciferase Reporter Assays

A firefly hLuc vector containing the TGFβ1 promoter (Promega), a pCMV renilla control and two anti-FOXO3 siRNAs, or a scrambled control (Origene) were transfected into U937 (Sundström and Nilsson, 1976) and MONO-MAC6 cells (Ziegler-Heitbrock et al., 1988). Results were analyzed at 48 hr using the Dual-Glo kit (Promega) and a Glomax reader (Promega).

Mice and DSS Colitis

C57BL/6 *Foxo3a*$^{MommeR1/MommeR1}$ (*Foxo3a*$^{-/-}$) mice were obtained from Emma Whitelaw (QIMR) and bred at the Australian National University (ANU). Colitis was induced in 8-week-old *Foxo3a*$^{-/-}$, *Foxo3a*$^{+/-}$, and *Foxo3a*$^{+/+}$ mice (littermates) using DSS (2% in drinking water, 7 days). Body weight was assessed daily, and colon length and weight on day 12. Blinded histological assessment was made using a standard scoring system (Dieleman et al., 1998), and cytokine expression quantified by qPCR from sections of paraffin-embedded colons. Approval was obtained from the ANU Animal Ethics Experimentation Committee.

Statistical Significance

Comparison of continuous variables between two groups was performed using Mann-Whitney or Wilcoxon signed-rank tests where indicated. Two-tailed tests were used as standard unless a specific hypothesis was tested. The alpha value was 0.05, unless corrected for multiple-testing.

SUPPLEMENTAL INFORMATION

Supplemental Information includes Extended Experimental Procedures, seven figures, and five tables, and a complete list of contributors from the UK IBD Genetics Consortium and can be found with this article online at http://dx.doi.org/10.1016/j.cell.2013.08.034.

ACKNOWLEDGMENTS

We gratefully thank the following: Cambridge BioResource (CBR) volunteers, the CBR staff for coordinating volunteer recruitment, and the CBR SAB for support; Emma Whitelaw (QIMR) for providing *Foxo3a*^{MommeR1} mice; Prof Adam Young (PI-NOAR) and Prof Deborah Symons (PI-ERAS) for collaboration; Alex W. Macharia, Sophie Uyoga, Carolyne Ndila, Emily Nyatichi, Metrine Tendwa, Johnstone Mkale, Adan Mohamed, Prophet Ingosi, and Mary Njoroge for DNA extraction at the KEMRI-Wellcome Trust Programme; and Gideon Nyutu, Kenneth Magua, and Ruth Mwarabu for database support. This work is published with permission from the director of KEMRI, supported by NIHR Biomedical Research centers in Cambridge and Manchester, and funded by the Wellcome Trust (program grant 083650/Z/07/Z, grants to J.C.L. 087007/Z/08/Z, C.A.A. 098051 and T.N.W. 091758/Z/10/Z), Arthritis Research UK and the Swiss Foundation for Medical Science (grant to S.V. PASMP3_134380). The Cambridge Institute for Medical Research is in receipt of Wellcome Trust Strategic Award (079895).

Received: April 12, 2013
Revised: July 8, 2013
Accepted: August 19, 2013
Published: September 12, 2013

REFERENCES

1000 Genomes Project Consortium, Abecasis, G.R., Altshuler, D., Auton, A., Brooks, L.D., Durbin, R.M., Gibbs, R.A., Hurles, M.E., and McVean, G.A. (2010). A map of human genome variation from population-scale sequencing. Nature *467*, 1061–1073.

Accili, D., and Arden, K.C. (2004). FoxOs at the crossroads of cellular metabolism, differentiation, and transformation. Cell *117*, 421–426.

Auffray, C., Sieweke, M.H., and Geissmann, F. (2009). Blood monocytes: development, heterogeneity, and relationship with dendritic cells. Annu. Rev. Immunol. *27*, 669–692.

Bain, C.C., Scott, C.L., Uronen-Hansson, H., Gudjonsson, S., Jansson, O., Grip, O., Guilliams, M., Malissen, B., Agace, W.W., and Mowat, A.M. (2013). Resident and pro-inflammatory macrophages in the colon represent alternative context-dependent fates of the same Ly6Chi monocyte precursors. Mucosal Immunol. *6*, 498–510.

Brunet, A., Bonni, A., Zigmond, M.J., Lin, M.Z., Juo, P., Hu, L.S., Anderson, M.J., Arden, K.C., Blenis, J., and Greenberg, M.E. (1999). Akt promotes cell survival by phosphorylating and inhibiting a Forkhead transcription factor. Cell *96*, 857–868.

Burgering, B.M., and Kops, G.J. (2002). Cell cycle and death control: long live Forkheads. Trends Biochem. Sci. *27*, 352–360.

Davignon, J.L., Hayder, M., Baron, M., Boyer, J.F., Constantin, A., Apparailly, F., Poupot, R., and Cantagrel, A. (2013). Targeting monocytes/macrophages in the treatment of rheumatoid arthritis. Rheumatology (Oxford) *52*, 590–598.

Dejean, A.S., Beisner, D.R., Ch'en, I.L., Kerdiles, Y.M., Babour, A., Arden, K.C., Castrillon, D.H., DePinho, R.A., and Hedrick, S.M. (2009). Transcription factor Foxo3 controls the magnitude of T cell immune responses by modulating the function of dendritic cells. Nat. Immunol. *10*, 504–513.

Dieleman, L.A., Palmen, M.J., Akol, H., Bloemena, E., Peña, A.S., Meuwissen, S.G., and Van Rees, E.P. (1998). Chronic experimental colitis induced by dextran sulphate sodium (DSS) is characterized by Th1 and Th2 cytokines. Clin. Exp. Immunol. *114*, 385–391.

Eijkelenboom, A., Mokry, M., de Wit, E., Smits, L.M., Polderman, P.E., van Triest, M.H., van Boxtel, R., Schulze, A., de Laat, W., Cuppen, E., and Burgering, B.M. (2013). Genome-wide analysis of FOXO3 mediated transcription regulation through RNA polymerase II profiling. Mol. Syst. Biol. *9*, 638.

Fadok, V.A., Bratton, D.L., Konowal, A., Freed, P.W., Westcott, J.Y., and Henson, P.M. (1998). Macrophages that have ingested apoptotic cells in vitro inhibit proinflammatory cytokine production through autocrine/paracrine mechanisms involving TGF-beta, PGE2, and PAF. J. Clin. Invest. *101*, 890–898.

Feldmann, M., and Maini, S.R. (2008). Role of cytokines in rheumatoid arthritis: an education in pathophysiology and therapeutics. Immunol. Rev. *223*, 7–19.

Franke, A., McGovern, D.P., Barrett, J.C., Wang, K., Radford-Smith, G.L., Ahmad, T., Lees, C.W., Balschun, T., Lee, J., Roberts, R., et al. (2010). Genome-wide meta-analysis increases to 71 the number of confirmed Crohn's disease susceptibility loci. Nat. Genet. *42*, 1118–1125.

Geissmann, F., Manz, M.G., Jung, S., Sieweke, M.H., Merad, M., and Ley, K. (2010). Development of monocytes, macrophages, and dendritic cells. Science *327*, 656–661.

Gomis, R.R., Alarcón, C., He, W., Wang, Q., Seoane, J., Lash, A., and Massagué, J. (2006). A FoxO-Smad synexpression group in human keratinocytes. Proc. Natl. Acad. Sci. USA *103*, 12747–12752.

Harada, Y., Harada, Y., Elly, C., Ying, G., Paik, J.H., DePinho, R.A., and Liu, Y.C. (2010). Transcription factors Foxo3a and Foxo1 couple the E3 ligase Cbl-b to the induction of Foxp3 expression in induced regulatory T cells. J. Exp. Med. *207*, 1381–1391.

Hedrick, S.M. (2009). The cunning little vixen: Foxo and the cycle of life and death. Nat. Immunol. *10*, 1057–1063.

Heliö, T., Halme, L., Lappalainen, M., Fodstad, H., Paavola-Sakki, P., Turunen, U., Färkkilä, M., Krusius, T., and Kontula, K. (2003). CARD15/NOD2 gene variants are associated with familially occurring and complicated forms of Crohn's disease. Gut *52*, 558–562.

Hindorff, L.A., MacArthur, J., Morales, J., Junkins, H.A., Hall, P.N., Klemm, A.K., and Manolio, T.A. (2013). A Catalog of Published Genome-Wide Association Studies. www.genome.gov/gwastudies.

Hugosson, E., Montgomery, S.M., Premji, Z., Troye-Blomberg, M., and Björkman, A. (2004). Higher IL-10 levels are associated with less effective clearance of Plasmodium falciparum parasites. Parasite Immunol. *26*, 111–117.

James, D., Young, A., Kulinskaya, E., Knight, E., Thompson, W., Ollier, W., and Dixey, J.; Early Rheumatoid Arthritis Study Group (ERAS), UK. (2004). Orthopaedic intervention in early rheumatoid arthritis. Occurrence and predictive factors in an inception cohort of 1064 patients followed for 5 years. Rheumatology (Oxford) *43*, 369–376.

Jostins, L., Ripke, S., Weersma, R.K., Duerr, R.H., McGovern, D.P., Hui, K.Y., Lee, J.C., Schumm, L.P., Sharma, Y., Anderson, C.A., et al.; International IBD Genetics Consortium (IIBDGC). (2012). Host-microbe interactions have shaped the genetic architecture of inflammatory bowel disease. Nature *491*, 119–124.

Kanehisa, M., and Goto, S. (2000). KEGG: kyoto encyclopedia of genes and genomes. Nucleic Acids Res. *28*, 27–30.

Kenyon, C.J. (2010). The genetics of ageing. Nature *464*, 504–512.

Kerdiles, Y.M., Stone, E.L., Beisner, D.R., McGargill, M.A., Ch'en, I.L., Stockmann, C., Katayama, C.D., and Hedrick, S.M. (2010). Foxo transcription factors control regulatory T cell development and function. Immunity *33*, 890–904.

Khor, B., Gardet, A., and Xavier, R.J. (2011). Genetics and pathogenesis of inflammatory bowel disease. Nature *474*, 307–317.

Krygier, D.S., Ko, H.H., and Bressler, B. (2009). How to manage difficult Crohn's disease: optimum delivery of anti-TNFs. Expert Rev. Gastroenterol. Hepatol. *3*, 407–415.

Lee, J.C., Lyons, P.A., McKinney, E.F., Sowerby, J.M., Carr, E.J., Bredin, F., Rickman, H.M., Ratlamwala, H., Hatton, A., Rayner, T.F., et al. (2011). Gene expression profiling of CD8+ T cells predicts prognosis in patients with Crohn disease and ulcerative colitis. J. Clin. Invest. *121*, 4170–4179.

Licastro, F., Candore, G., Lio, D., Porcellini, E., Colonna-Romano, G., Franceschi, C., and Caruso, C. (2005). Innate immunity and inflammation in ageing: a key for understanding age-related diseases. Immun. Ageing *2*, 8.

Litvak, V., Ratushny, A.V., Lampano, A.E., Schmitz, F., Huang, A.C., Raman, A., Rust, A.G., Bergthaler, A., Aitchison, J.D., and Aderem, A. (2012). A FOXO3-IRF7 gene regulatory circuit limits inflammatory sequelae of antiviral responses. Nature *490*, 421–425.

Lundberg, A.M., Drexler, S.K., Monaco, C., Williams, L.M., Sacre, S.M., Feldmann, M., and Foxwell, B.M. (2007). Key differences in TLR3/poly I:C signaling and cytokine induction by human primary cells: a phenomenon absent from murine cell systems. Blood *110*, 3245–3252.

Malaguarnera, L., and Musumeci, S. (2002). The immune response to Plasmodium falciparum malaria. Lancet Infect. Dis. *2*, 472–478.

McClellan, J., and King, M.C. (2010). Genetic heterogeneity in human disease. Cell *141*, 210–217.

McKinney, E.F., Lyons, P.A., Carr, E.J., Hollis, J.L., Jayne, D.R., Willcocks, L.C., Koukoulaki, M., Brazma, A., Jovanovic, V., Kemeny, D.M., et al. (2010). A CD8+ T cell transcription signature predicts prognosis in autoimmune disease. Nat. Med. *16*, 586–591, 1p, 591.

Modur, V., Nagarajan, R., Evers, B.M., and Milbrandt, J. (2002). FOXO proteins regulate tumor necrosis factor-related apoptosis inducing ligand expression. Implications for PTEN mutation in prostate cancer. J. Biol. Chem. *277*, 47928–47937.

Mulherin, D., Fitzgerald, O., and Bresnihan, B. (1996). Synovial tissue macrophage populations and articular damage in rheumatoid arthritis. Arthritis Rheum. *39*, 115–124.

Musso, T., Espinoza-Delgado, I., Pulkki, K., Gusella, G.L., Longo, D.L., and Varesio, L. (1990). Transforming growth factor beta downregulates interleukin-1 (IL-1)-induced IL-6 production by human monocytes. Blood *76*, 2466–2469.

Nakae, J., Oki, M., and Cao, Y. (2008). The FoxO transcription factors and metabolic regulation. FEBS Lett. *582*, 54–67.

Ouyang, W., Beckett, O., Ma, Q., Paik, J.H., DePinho, R.A., and Li, M.O. (2010). Foxo proteins cooperatively control the differentiation of Foxp3+ regulatory T cells. Nat. Immunol. *11*, 618–627.

Pritchard, J.K., Stephens, M., and Donnelly, P. (2000a). Inference of population structure using multilocus genotype data. Genetics *155*, 945–959.

Rainbow, D.B., Esposito, L., Howlett, S.K., Hunter, K.M., Todd, J.A., Peterson, L.B., and Wicker, L.S. (2008). Commonality in the genetic control of Type 1 diabetes in humans and NOD mice: variants of genes in the IL-2 pathway are associated with autoimmune diabetes in both species. Biochem. Soc. Trans. *36*, 312–315.

Rennick, D.M., Fort, M.M., and Davidson, N.J. (1997). Studies with IL-10-/- mice: an overview. J. Leukoc. Biol. *61*, 389–396.

Rivollier, A., He, J., Kole, A., Valatas, V., and Kelsall, B.L. (2012). Inflammation switches the differentiation program of Ly6Chi monocytes from antiinflammatory macrophages to inflammatory dendritic cells in the colon. J. Exp. Med. *209*, 139–155.

Seoane, J., Le, H.V., Shen, L., Anderson, S.A., and Massagué, J. (2004). Integration of Smad and forkhead pathways in the control of neuroepithelial and glioblastoma cell proliferation. Cell *117*, 211–223.

Sundström, C., and Nilsson, K. (1976). Establishment and characterization of a human histiocytic lymphoma cell line (U-937). Int. J. Cancer *17*, 565–577.

Symmons, D.P., and Silman, A.J. (2003). The Norfolk Arthritis Register (NOAR). Clin. Exp. Rheumatol. *21*(5, Suppl 31), S94–S99.

Tran, T.H., Day, N.P., Nguyen, H.P., Nguyen, T.H., Tran, T.H., Pham, P.L., Dinh, X.S., Ly, V.C., Ha, V., Waller, D., et al. (1996). A controlled trial of artemether or quinine in Vietnamese adults with severe falciparum malaria. N. Engl. J. Med. *335*, 76–83.

Watkins, S.K., Zhu, Z., Riboldi, E., Shafer-Weaver, K.A., Stagliano, K.E., Sklavos, M.M., Ambs, S., Yagita, H., and Hurwitz, A.A. (2011). FOXO3 programs tumor-associated DCs to become tolerogenic in human and murine prostate cancer. J. Clin. Invest. *121*, 1361–1372.

Wellcome Trust Case Control Consortium. (2007). Genome-wide association study of 14,000 cases of seven common diseases and 3,000 shared controls. Nature *447*, 661–678.

Wildey, G.M., and Howe, P.H. (2009). Runx1 is a co-activator with FOXO3 to mediate transforming growth factor beta (TGFbeta)-induced Bim transcription in hepatic cells. J. Biol. Chem. *284*, 20227–20239.

Williams, T.N., Wambua, S., Uyoga, S., Macharia, A., Mwacharo, J.K., Newton, C.R., and Maitland, K. (2005). Both heterozygous and homozygous alpha+ thalassemias protect against severe and fatal Plasmodium falciparum malaria on the coast of Kenya. Blood *106*, 368–371.

Yang, J.Y., Zong, C.S., Xia, W., Yamaguchi, H., Ding, Q., Xie, X., Lang, J.Y., Lai, C.C., Chang, C.J., Huang, W.C., et al. (2008). ERK promotes tumorigenesis by inhibiting FOXO3a via MDM2-mediated degradation. Nat. Cell Biol. *10*, 138–148.

Youngson, N.A., Vickaryous, N., van der Horst, A., Epp, T., Harten, S., Fleming, J.S., Khanna, K.K., de Kretser, D.M., and Whitelaw, E. (2011). A missense mutation in the transcription factor Foxo3a causes teratomas and oocyte abnormalities in mice. Mamm. Genome *22*, 235–248.

Ziegler-Heitbrock, H.W., Thiel, E., Fütterer, A., Herzog, V., Wirtz, A., and Riethmüller, G. (1988). Establishment of a human cell line (Mono Mac 6) with characteristics of mature monocytes. Int. J. Cancer *41*, 456–461.

EXTENDED EXPERIMENTAL PROCEDURES

Candidate Gene Identification

81 genes implicated in IL-2 and IL-7 signaling were identified from published literature and pathway libraries (Biocarta, http://www.biocarta.com; KEGG (Kanehisa and Goto, 2000) (Table S1). 1134 SNPs within these genes (including 2 kb on either side to encompass regulatory regions) and present on the Affymetrix 500K SNP array were included.

Patient Subgroups

Subgroups of patients with ''aggressive'' or ''indolent'' CD were identified from a CD GWAS cohort (Wellcome Trust Case Control Consortium, 2007). Aggressive CD was defined as disease that had required $\geq$2 immunomodulators and/or intestinal resections (treatments reserved for frequently-flaring or complicated CD). Indolent CD was defined as disease of greater than 4 years duration, which had not required any immunomodulators or intestinal resections. Patients who did not meet either criteria, or those where additional immunomodulators or surgery were required for drug intolerance or complications of earlier surgery respectively, were excluded.

GWAS Reanalysis and Replication

Single-marker allelic association analysis was performed, using post-QC genotype calls (Wellcome Trust Case Control Consortium, 2007). Samples were excluded if they were of non-Northern European ancestry using principal components. The association analysis was conducted in PLINK (http://pngu.mgh.harvard.edu/~purcell/plink) using Cochran-Armitage trend tests. The genomic control inflation factor was 1.04. Three independent replication cohorts were identified (Table S3). Replication genotyping was performed using TaqMan predesigned SNP genotyping assays (Applied Biosciences) in cohorts 1 and 2, called by two independent operators, and post-QC genotype calls (Shah et al., 2012) from the Illumina Immunochip (Cortes and Brown, 2011) in cohort 3. Statistical significance in the replication cohorts was determined using Fisher's exact test.

Population Structure

3 independent methods were used to determine whether cryptic population structure might underlie the association we observe.

First, the genomic control inflation factor was calculated (λ_{GC}). This represents the confounding effect of population structure on the association results, and should be 1.0 if no structure exists. In the primary cohort the λ_{GC} was 1.04, which is well below the level for which correction is conventionally required, and suggests that the effect of cryptic population structure is negligible.

Second, we used *structure* (Pritchard et al., 2000a), a model-based clustering method for determining population structure from genotype data, and STRAT, a companion program that incorporates the results from *structure* to adjust for population structure in association analysis. These analyses suggested that the contribution of population structure to our results is negligible because the proportion of the cohort assigned to each population was symmetric, and most individuals were admixed across iterations—as typically occurs when little / no population structure exists (Pritchard et al., 2000b). Further evidence that there was little / no population structure was obtained by applying the Evanno method to the *structure* analysis results (Evanno et al., 2005). This was done to determine the true number of clusters present, and suggested that if any population structure exists, it is best explained by there being at most 2 clusters within the data (although the technique is unable to validate if 1 cluster is an even better fit). Using this result, we then reran the association analysis in STRAT to correct for the presence of 2 possible clusters. This showed that the association of rs12212067: T > G with prognosis remained, and that the significance of the result was negligibly affected ($p = 8.0 \times 10^{-4}$).

Third, a Breslow Day test was performed to examine the homogeneity of odds ratios across the 4 CD cohorts. This confirmed that there was no significant heterogeneity in the association ($p = 0.79$), suggesting that any population structure would have to be consistent across 4 independent cohorts, sampled from several sites within the UK and New Zealand, in order to drive the association.

Linkage Disequilibrium around rs12212067

A 2 Mb region from Pilot 1 of the 1000 Genomes Project (1000 Genomes Project Consortium, 2010) was analyzed in PLINK to identify SNPs in LD with rs12212067 ($r^2 > 0.5$).

Cambridge BioResource

Functional experiments were performed using samples from a genotype-selectable bioresource (Cambridge BioResource [CBR], http://www.cambridgebioresource.org.uk). Disease-free individuals of appropriate genotype were identified, consented and venesected by CBR staff (50 mls venous blood). Investigators were blinded to the genotype of samples until study completion. For experiments requiring comparison between two genotypes, samples were paired and age and sex matched.

Allele-Specific Expression

A clone-based allele-specific expression assay was performed using a described method (Rainbow et al., 2008). In brief, positively-selected $CD14^+$ monocytes (Lyons et al., 2007) (from heterozygotes at rs12212067) were stimulated for 6 hr (LPS, 100 ng/ml), or left unstimulated. Nested primers flanking rs12212067 were used to amplify complementary DNA (cDNA; synthesized from pre-mRNA) and genomic DNA (gDNA). Forward, GTAGCTGTGGGACCTTGCAT; Reverse, CACATGTAGGAAGGGCCTGT (product length

1,045 bp); Nested forward, TCCAGCCCCTTTTTACCAC; Nested reverse, TGTTCAGAAAGCAGGCAAGT (product length 493 bp). Amplicons were gel purified, cloned into vectors containing a kanamycin-resistance cassette (Zero Blunt(R) TOPO(R) Cloning kit, Invitrogen) and transfected into chemically competent *E.coli*, which were grown on kanamycin-containing LB agar. 96 colonies per individual per condition were genotyped (TaqMan, Applied Biosystems).

Flow Cytometry

Flow cytometry was performed using a CyAN ADP flow cytometer (Beckman Coulter). Antibodies are listed in Table S5B. For intracellular cytokine staining, PBMC were stimulated for 6 hr (LPS, 100 ng/ml) with 1 μl/ml GolgiStop and 1 μl/ml GolgiPlug (BD) prior to fixation and permeabilisation (Cytofix/Cytoperm kit, PharMingen). A ligand-blocking control was used. Data were analyzed using FlowJo software (TreeStar).

Cell Stimulations

1×10^6 cells in 1 ml cell-culture media (RPMI-1640, 10% decomplemented fetal bovine serum, penicillin [100 u/ml], streptomycin [100 μg/ml] and L-glutamine [2 mM]) were stimulated in flat-bottomed 24-well plates (37°C, 5% CO_2). 50 μl of stimulus or control (phosphate buffered saline) was added to produce the concentrations shown: *E.coli*-derived LPS (10 ng/ml, 100 ng/ml; Sigma), Flagellin (5 μg/ml; Invivogen), Poly(I:C) (5 μg/ml; Invivogen), CpG DNA (5 μg/ml; Invivogen), Pam3Cys4 (10 μg/ml; Invivogen), TGFβ1 (1.25 ng/ml; Peprotech), TGFβ1-neutralising monoclonal antibody (1 μg/ml; Abcam). For experiments involving autologous neutrophils, 5×10^5 were added either immediately following positive selection (Lyons et al., 2007) (nonapoptotic) or following induction of apoptosis (254 nm UV light [10 min] followed by 1 hr incubation; apoptotic). Average percentages of 7-AAD$^+$, Annexin V$^+$ neutrophils were 3% and 62% respectively, with < 3% necrosis (assessed by trypan blue exclusion).

Cytokine Assays

TNFα and IL-10 were quantified by cytometric bead array (BD) for initial PBMC stimulations, by ELISA for subsequent experiments (Quantikine ELISA; TNFα, IL-10 and TGFβ1) and by Meso Scale Discovery immunoassays for other cytokines (GMCSF, IL-1β, IL-2, IL-4, IL-5, IL-6, IL-8 and IL-12p70). All assessments were performed in triplicate.

Immunofluorescence

Stimulated monocytes (LPS, 100 ng/ml) were plated onto poly-L-lysine-coated coverslips at specific times, fixed (4% paraformaldehyde) and blocked (2% gelatin, 37°C, 1 hr). FOXO3 was stained using a primary antibody (Cell Signaling) and a secondary AF594-conjugated antibody (Molecular Signaling). Coverslips were mounted using Mowiol containing Hoechst dye. Images were captured (4 hpf per individual per time point) on a Zeiss LSM510 META Confocal Microscope and analyzed in a blinded fashion with Volocity software (Perkin Elmer). Cycloheximide was used at 5 μg/ml.

Apoptosis

Apoptosis was quantified following 24 hr stimulation (LPS, 100 ng/ml) by flow cytometry (7-AAD, Annexin V) and by quantification of mono- and oligonucleosomes in the cytoplasm and supernatants (Cell Death Detection ELISAPlus, Roche).

ChIP-qPCR

ChIP-qPCR was performed using a commercial ChIP kit (Abcam) and aliquots of 3×10^6 stimulated monocytes (LPS, 100 ng/ml, 12 hr). Chromatin was sheared by water-bath sonication (30 s cycles [on/off], 5 min; Bioruptor, Diagenode). FOXO3 was immunoprecipitated using a ChIP-grade antibody (Abcam). Positive (input) and negative (polyclonal IgG; BD Biosciences) controls were used. Quantitative PCR was performed for a region of the *TGFβ1* promoter predicted to contain a FOXO3-binding site (Forward, GCTTCTGTCCTTTCTAGG; Reverse, CAGCCTCCTGTCACTCAACA). 6 positive and 5 negative controls were used—all primers and genomic regions previously validated and published in Eijkelenboom et al., 2013. Positive controls: PDGFRA-5 kb-DS-intron, HMGA-129 kb-DS-intron, KC6-210 kb-US, KLF6-37 kb-DS-intron, CYB5a-10 kb-DS-intron, MSTN-32 kb-US. Negative controls: Neg. control HBB, Neg. control GAPDH, Neg. control MB, Neg. control 1, Neg. control 2. Primer sequences available in Table S3 from Eijkelenboom et al., 2013. Input DNA was standardized (5 ng) and the results normalized to the negative control pull-down.

Luciferase Assay

Two monocyte cell lines, U-937 (Sundström and Nilsson, 1976) and MONO-MAC6 (Ziegler-Heitbrock et al., 1988) (DSMZ, http://www.dsmz.de) were cultured in media supplemented with HYBRI-MAX (Sigma-Aldrich). Cells were seeded at 2×10^5 cells/ml and cultured overnight without antibiotics before transient transfection with a firefly pGL4.14 hLuc vector containing the *TGFβ1* promoter (666 ng/ml, Promega), a pCMV renilla luciferase control vector (6.6 ng/ml), and one of two *FOXO3A* siRNAs, or a scrambled control (66 nM/ml, Origene) using lipofectamine 2000 (Invitrogen). Primers: Forward: 5′AAAGCTAGCCACGTGGCGG CCCCTGGGCA; Reverse: 5′AAAAGATCTACCGGCTGGGTCGGCAGGGGGT (product size 1,000 bp).

Firefly and renilla luciferase activities were assessed at 48 hr using the Dual-Glo kit and a Glomax reader (Promega).

Mice and DSS Colitis

Foxo3a$^{MommeR1/MommeR1}$ mice were obtained from Emma Whitelaw (Queensland Institute for Medical Research) and bred at the Australian National University (ANU). Colitis was induced in 8 week old *Foxo3*$^{MommeR1/MommeR1}$ mice and hemizygous and wild-type littermate controls using DSS in drinking water (2%, 7 days). After 7 days, normal drinking water was reinstated. Body weight was assessed daily, and colon length and weight on day 12. Blinded histological assessment was performed using a standard scoring system (Dieleman et al., 1998) and cytokine expression was assessed by quantitative RT-PCR (TaqMan predesigned qPCR assays, Applied Biosciences) using mRNA extracted from sections of paraffin-embedded colons using an RNEasy FFPE kit (QIAGEN). Experimental approval was obtained from the ANU Animal Ethics Experimentation Committee.

RA Cohorts

Deatils of the Norfolk Arthritis Register (NOAR) and Early Rheumatoid Arthritis Study (ERAS) have been published previously (Symmons and Silman, 2003; James et al., 2004). RA patients from NOAR or ERAS with at least one set of hand and feet radiographs at recruitment or during a prospective 5 year follow-up period were genotyped using the Illumina Immunochip (Cortes and Brown, 2011) or Sequenom MassArray respectively. 1071 RA patients in NOAR and 382 RA patients in ERAS with nonmissing genotype were identified, corresponding to 1,696 and 1,915 X-rays respectively—all of which were assessed using the Larsen score (Larsen, 1995). To incorporate multiple records per patient over time, Larsen score was considered as a continuous time-dependent longitudinal trait. Analysis was performed for the first five years of follow-up. Generalized Linear Latent and Mixed Modeling (GLLAMM) with discrete random effects and three latent classes to appropriately fit the nonnormal distribution of Larsen scores was used to assess the association between Larsen score and the minor (G) allele of rs12212067, assuming additivity on the log-odds scale. Separate linear and quadratic terms of disease duration were fit for the three latent classes to allow for differences between the latent classes in the nonlinear trajectories of Larsen score over time. The association analysis was adjusted for patient's age at baseline and the square of it, to allow for a nonlinear relationship.

Malaria Cohorts

Details of the Kenyan and Vietnamese malaria cohorts have been published previously (Tran et al., 1996; Williams et al., 2005). In brief, both contained unrelated patients who required hospital admission for *P. falciparum* parasitaemia complicated by features of severe malaria (Kenyan n = 1,340, Vietnamese n = 223) and ethnically matched controls (Kenyan n = 2,436, Vietnamese n = 653). Genotyping was performed using TaqMan predesigned SNP genotyping assays (Applied Biosciences). Statistical significance was determined using Fisher's exact test (one-tailed).

Statistical Analysis

Comparison of continuous variables between 2 groups was performed using Mann-Whitney tests or Wilcoxon signed-rank tests as appropriate. Two-tailed tests were used as standard unless a specific hypothesis was being tested. The alpha value was 0.05, unless corrected for multiple-testing.

SUPPLEMENTAL REFERENCES

Barrett, J.C., Fry, B., Maller, J., and Daly, M.J. (2005). Haploview: analysis and visualization of LD and haplotype maps. Bioinformatics *21*, 263–265.

Cortes, A., and Brown, M.A. (2011). Promise and pitfalls of the Immunochip. Arthritis Res. Ther. *13*, 101.

Evanno, G., Regnaut, S., and Goudet, J. (2005). Detecting the number of clusters of individuals using the software STRUCTURE: a simulation study. Mol. Ecol. *14*, 2611–2620.

Johnson, A.D., Handsaker, R.E., Pulit, S.L., Nizzari, M.M., O'Donnell, C.J., and de Bakker, P.I. (2008). SNAP: a web-based tool for identification and annotation of proxy SNPs using HapMap. Bioinformatics *24*, 2938–2939.

Larsen, A. (1995). How to apply Larsen score in evaluating radiographs of rheumatoid arthritis in long-term studies. J. Rheumatol. *22*, 1974–1975.

Lyons, P.A., Koukoulaki, M., Hatton, A., Doggett, K., Woffendin, H.B., Chaudhry, A.N., and Smith, K.G.C. (2007). Microarray analysis of human leucocyte subsets: the advantages of positive selection and rapid purification. BMC Genomics *8*, 64.

Pritchard, J.K., Stephens, M., Rosenberg, N.A., and Donnelly, P. (2000b). Association mapping in structured populations. Am. J. Hum. Genet. *67*, 170–181.

Shah, T.S., Liu, J.Z., Floyd, J.A., Morris, J.A., Wirth, N., Barrett, J.C., and Anderson, C.A. (2012). optiCall: a robust genotype-calling algorithm for rare, low-frequency and common variants. Bioinformatics *28*, 1598–1603.

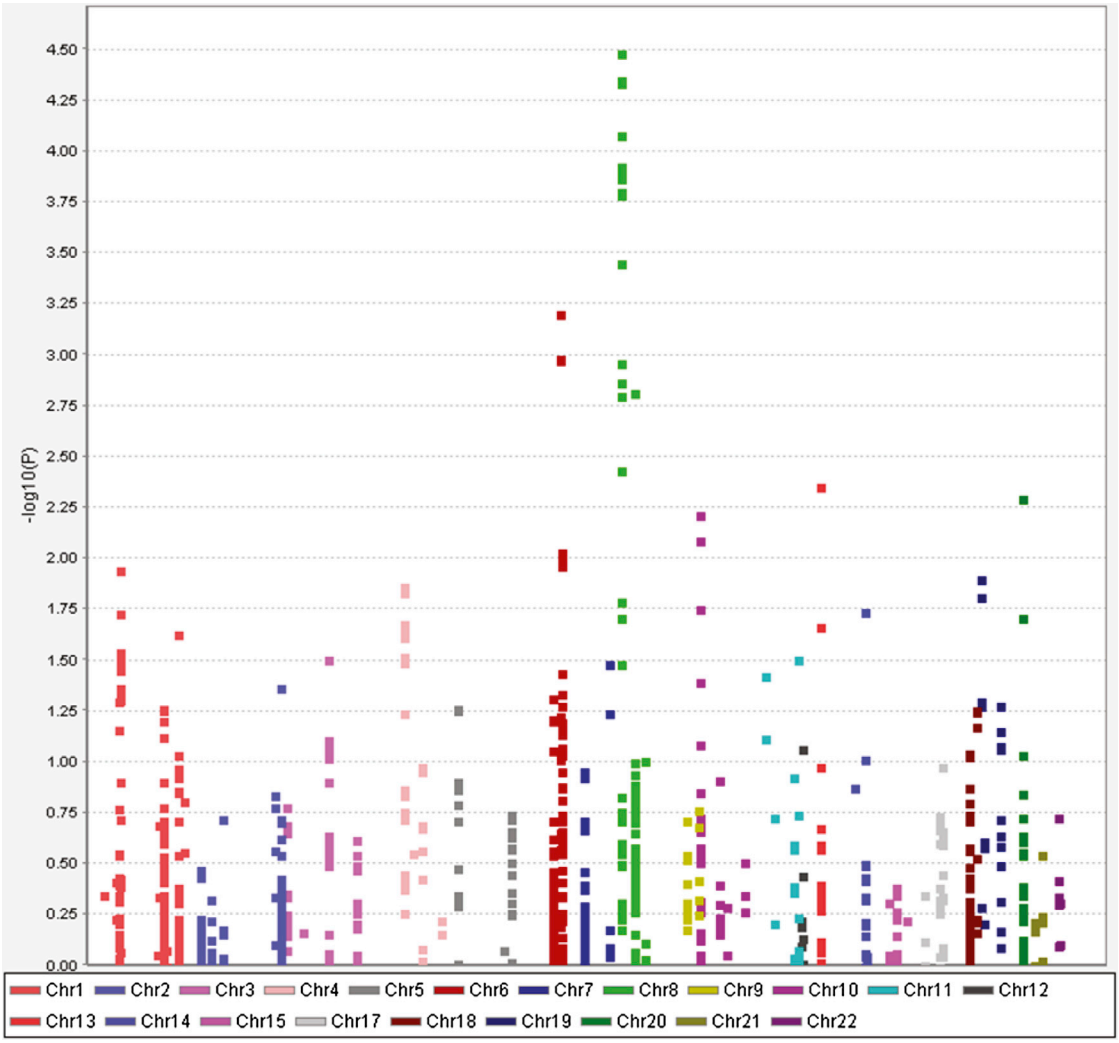

Figure S1. Cochran-Armitage Plot of Candidate Gene Association Analysis, Related to Table 1

Cochran Armitage plot of –log(10) p values against chromosomal position for the candidate gene association analysis results (primary cohort only—668 aggressive CD, 389 indolent CD). Each point represents a SNP. 1134 SNPs within 81 genes in the IL-2 and IL-7 signaling pathways were included in the analysis. Manhattan plot generated using Haploview (Barrett et al., 2005).

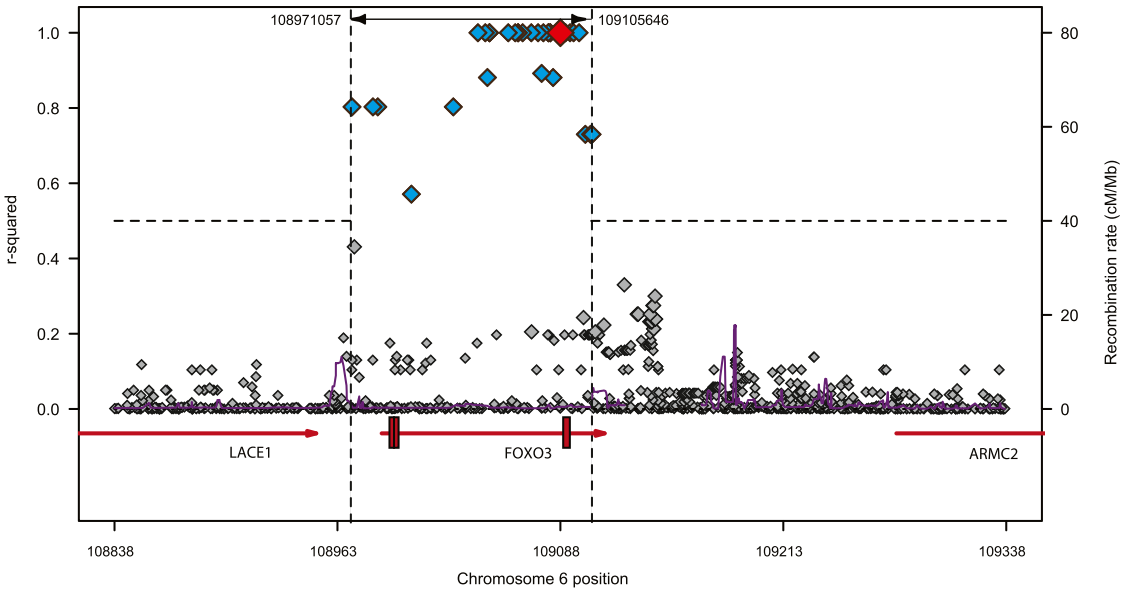

Figure S2. Linkage Disequilibrium around rs12212067 Is Limited to *FOXO3A*, Related to Figure 1

Regional LD plot—adapted from a plot generated using SNP Annotation and Proxy software (Johnson et al., 2008)—demonstrating linkage disequilibrium around rs12212067. Each SNP is represented by a diamond and its position is plotted against its r^2 value with rs12212067. Those with $r^2 \geq 0.5$ are filled blue. Rs12212067 is represented by the red diamond. The dotted lines indicate a region of LD where $r^2 \geq 0.5$. The horizontal arrowed lines below represent the genes in this region, with the arrows indicating the direction of transcription and the exons in *FOXO3A* shown as red bars. The purple line indicates the recombination rate.

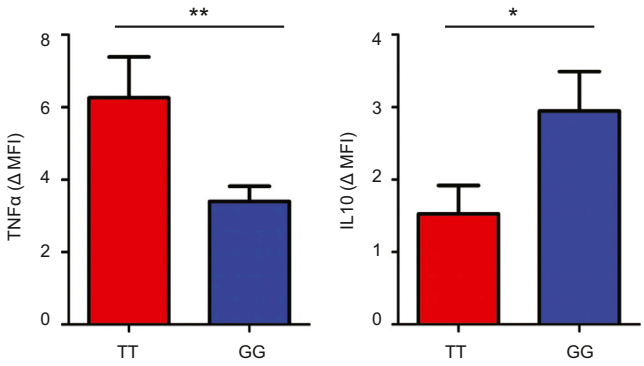

Figure S3. Genotype at rs12212067 Correlates with TNFα and IL-10 Production in Stimulated Monocytes, Related to Figure 1

The amount of TNFα and IL-10 produced by monocytes following LPS stimulation (6 hr) was quantified by intracellular flow cytometry. The increase in mean fluorescence intensity (compared with autologous unstimulated monocytes) is shown—stratified by genotype (GG, minor allele homozygotes; TT, major allele homozygotes). n = 20, data are represented as mean ± SEM. *$p < 0.05$, **$p < 0.01$.

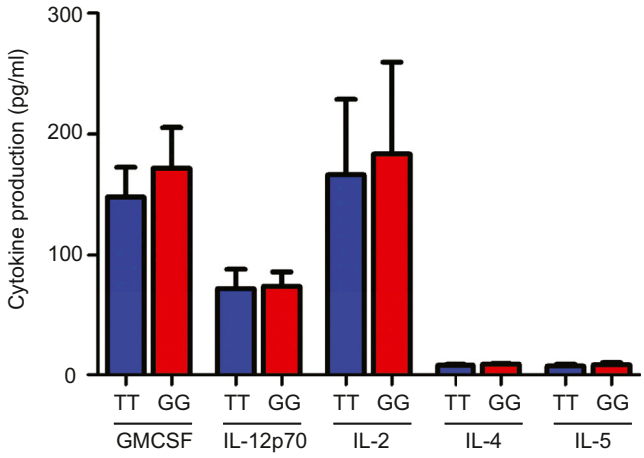

Figure S4. Genotype at rs12212067 Does Not Alter Monocyte Production of GMCSF, IL-12p70, IL-2, IL-4, or IL-5, Related to Figure 1

GMCSF, IL-12p70, IL-2, IL-4 and IL-5 production by purified monocytes from minor and major allele homozygotes following 24 hr' stimulation with LPS (same samples as used in Figures 1D and 1F), n = 22. None of the comparisons were significantly different (all $p \geq 0.05$). Data are represented as mean ± SEM.

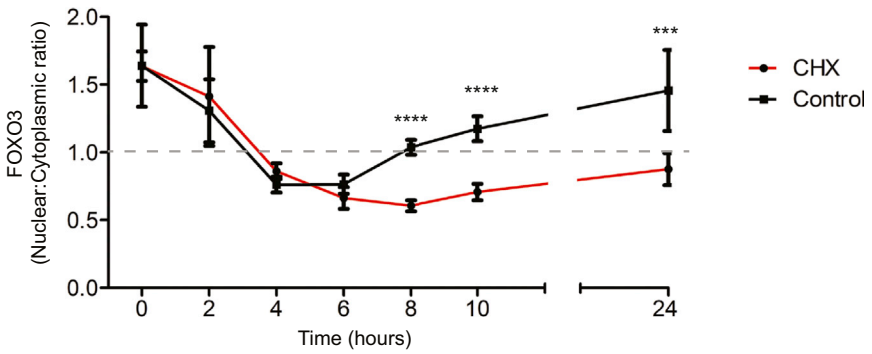

Figure S5. Inhibition of Protein Synthesis Retards the Recovery of Nuclear FOXO3 in Stimulated Monocytes, Related to Figure 2

The effect of cycloheximide (CHX, 5 μg/ml) upon the ratio of nuclear:cytoplasmic FOXO3 in stimulated monocytes was assessed by immunofluorescence. Quantification of immunofluorescence was performed by an independent observer blinded to the experimental details. The dotted line indicates the transition from higher signal in nucleus (above) to higher signal in cytoplasm (below). All live cells in 4 high-powered fields assessed at each time point. Data are represented as mean ± SEM, ***$p < 0.001$, ****$p < 0.0001$.

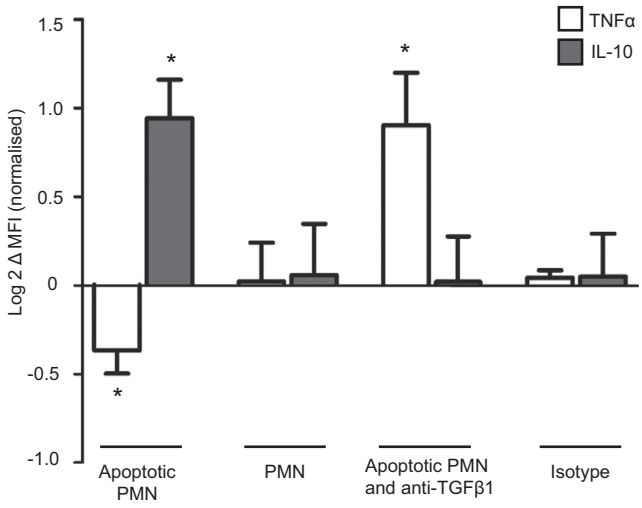

Figure S6. Apoptotic Cells Modulate Inflammatory Responses in a TGFβ1-Dependent Manner, Related to Figure 4

The effect of coincubating autologous apoptotic neutrophils or autologous nonapoptotic neutrophils (PMN) upon TNFα and IL-10 production by LPS-stimulated monocytes, assessed using flow cytometry. Data are $\log_2$ transformed following normalization, Wilcoxon signed-rank test; n = 6, data represented as mean ± SEM, *$p < 0.05$.

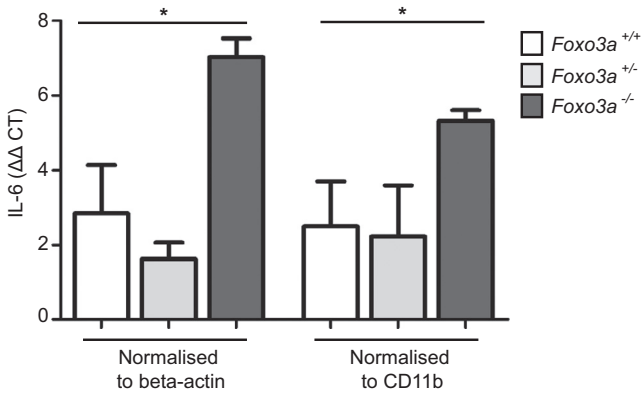

Figure S7. Loss of *Foxo3a* Activity Leads to Increased IL-6 Expression in the Colon in a Mouse Model of Colitis, Related to Figure 5

Colitis was induced in littermate *Foxo3a*$^{-/-}$, *Foxo3a*$^{+/-}$ and *Foxo3*$^{+/+}$ mice using 2% DSS in drinking water for 7 days. Mice were killed on day 12 and colons were removed and paraffin-embedded. Quantitative PCR of IL-6 mRNA extracted from paraffin-embedded sections. Representative data are shown for one of two experiments each with 5 mice per group, Mann Whitney test. Data are represented as mean ± SEM, *$p < 0.05$.